PIONS AND OTHER HADRONIC DEGREES OF FREEDOM IN NUCLEI*)

W. Weise
Institute of Theoretical Physics
University of Regensburg
D-8400 Regensburg, FR Germany

*) Work supported in part by Bundesministerium für Forschung und Technologie (grant MEP-33-REA) and by Deutsche Forschungsgemeinschaft (grant We 655/7-6).

LECTURE 1

1. Introduction

The traditional picture of the nucleus in low energy nuclear physics is that of an interacting many-body system of structureless, pointlike protons and neutrons. Here low energy nuclear physics is understood to be the region of excitation energies ΔE smaller than the Fermi energy ($\varepsilon_F \simeq 30 - 40$ MeV) and momentum transfers $\Delta q \lesssim 1/R$, where R is the nuclear radius.

The situation changes as ΔE and/or Δq is increased up to several hundreds of MeV, the domain of intermediate energy physics. At this point explicit mesonic degrees of freedom become directly visible. The pion, in particular, is of fundamental importance. With its small mass of $m_\pi = 140$ MeV it is by far the lightest of all mesons. It is the generator of the long range nucleon-nucleon interaction. The pion Compton wavelength, $\lambda\!\!\!^{-}_\pi = \hbar/m_\pi c = 1.4$ fm, defines the length scale of nuclear physics.

As mesons become important, nucleons begin to reveal their intrinsic structure. Inseparably connected with pionic degrees of freedom is the role of the $\Delta(1232)$, the spin 3/2-isospin 3/2 isobar reached from the nucleon by a strong spin-isospin transition at an excitation energy $\Delta E = M_\Delta - M \simeq 300$ MeV, the Δ-nucleon mass difference.

In these lectures, the position will be taken that the nucleus consists of nucleons and their excited states (primarily the $\Delta(1232)$) which communicate by exchange of mesons (in particular: the pion). Such a description has turned out to be quite successful in correlating various phenomena and data at intermediate energies, remarkably though without the need, so far, for explicit reference to underlying quark degrees of freedom. This progress has gone parallel with the similarly successful meson exchange phenomenology of nucleon-nucleon forces at long and intermediate distances ($r \gtrsim 0.8$ fm). A survey of the rapid experimental and theoretical progress in meson-nuclear physics can be obtained by consulting the conference proceedings [1] and [2], and recent reviews in ref. [3-6].

While there may not be a need for explicitly invoking quark degrees of freedom in nuclei up to a few hundred MeV of excitation energy, there is an obvious necessity to understand the phenomenological input into nuclear forces from a more fundamental (quark-gluon dynamical) point of view. Attempts to establish relationships of this kind are still at their very beginning, but there is little doubt that activities in this direction will constitute a substantial part of intermediate energy physics research in coming years. Some of the developments will be touched in these lectures, though not at a very detailed level.

2. The Nucleon-Nucleon Interaction

2.1 Survey: Mesons and the Nuclear Force

The nucleon-nucleon interaction has been a problem of fundamental interest and challenge ever since Yukawa's pioneering work in 1935. The problem is still unsolved: it is yet impossible to derive nuclear forces directly from Quantum Chromodynamics, the theory of strong interactions. However, over the years, meson exchange models have established a highly successful phenomenology.

A schematic picture of the nucleon-nucleon potential in the $^1S_0$ state is shown in Fig. 1. At distances of the order of the pion Compton wave length and beyond, the one-pion exchange interaction dominates. At intermediate distances two-pion exchange mechanisms become important. The lowest angular momentum carried by the exchanged pion pair is $J^\pi = 0^+$, together with isospin I = 0 in accordance with the symmetry of the $(\pi\pi)$ state. The corresponding $(\pi\pi)$ mass spectrum has a broad distribution. In one-boson exchange models, this is usually prametrized in terms of an effective "σ" boson with a mass between 400 and 600 MeV.

Furthermore, two interacting pions in a $J^\pi = 1^-$ and isospin I = 1 state resonate strongly to form the ρ meson with a mass $m_\rho = 770$ MeV.

Down to about $r \gtrsim 0.8$ fm, two-pion exchange processes can be treated rather accurately using dispersion relation methods, such as in the Paris [7] or Stony Brook [8] NN-interaction, or in refined versions of the Bonn potential [9]. At shorter distances ($r \lesssim 0.8$ fm), the understanding of the NN force is more or less on phenomenological grounds only. In a one-boson exchange description (e.g. of the Bonn [10] or Nijmegen [11] groups), the short-range repulsion is simulated by exchange of a strongly coupled ω meson ($J^\pi = 1^-$, I = 0) with a mass $m_\omega = 783$ MeV.

Both ρ and ω exchange take place primarily at distances comparable to their Compton wavelengths $m_\rho^{-1} \simeq m_\omega^{-1} \sim 1/4$ fm, which is the same order of magnitude as the nucleon size itself. It is therefore difficult to imagine how a ρ or ω meson can travel freely between two nucleons. One has to expect that there is a massive influence of finite-size cutoffs. In any case, one probably has to interpret these short-range vector meson exchanges as phenomenological representations of complex mechanisms taking place at the level of quarks and gluons, once two nucleons approach each other at distances so small that their quark cores most likely overlap.

Nevertheless, the one- and two-boson exchange phenomenology provides a quantitatively successful description of NN scattering data and deuteron properties. We summarize properties of the exchanged mesons and meson-nucleon coupling constants in table 1. The coupling constants refer to meson-nucleon effective Lagrangians of the following types:

Scalar: $$\mathcal{L}_s = g_s \bar{\psi}(x)\, \psi(x)\, \phi_s(x) \,, \tag{2.1a}$$

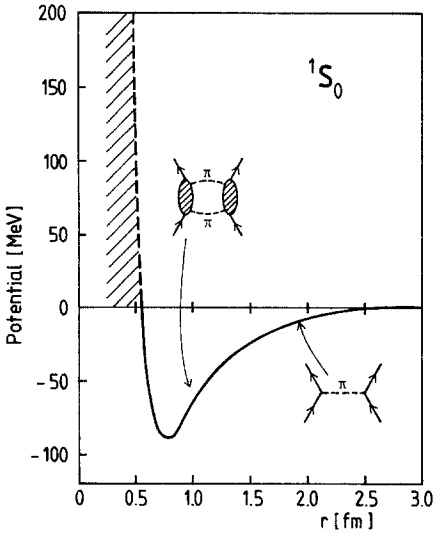

Figure 1: Schematic picture of the NN interaction in the $^1S_0$ channel

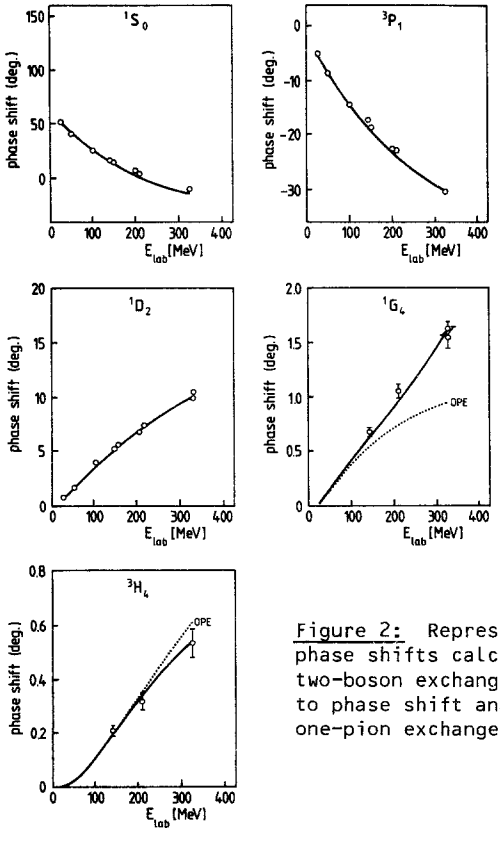

Figure 2: Representative selection of NN phase shifts calculated with a one- and two-boson exchange model [9], as compared to phase shift analysis of NN data. OPE: one-pion exchange only.

Pseudoscalar: $$\mathcal{L}_p = g_p \bar{\psi}(x)\, i\gamma_5\, \psi(x)\, \phi_p(x), \qquad (2.1b)$$

Vector: $$\mathcal{L}_V = \left[g_V \bar{\psi}(x)\gamma_\mu \psi(x) + (g_T/2M)\,\bar{\psi}(x)\sigma_{\mu\nu}\psi(x)\partial^\nu\right] V^\mu(x). \qquad (2.1c)$$

Here $\psi(x)$ are the nucleon Dirac spinor fields, and we follow the Bjorken and Drell conventions for metric and Dirac-γ matrices [+)]. The ϕ_s, ϕ_p and V^μ refer to scalar, pseudoscalar and vector meson fields. For isovector mesons the isospin dependence enters in the form $\vec{\tau}\cdot\vec{\phi}$ or $\vec{\tau}\cdot\vec{V}^\mu$, respectively, where $\vec{\tau} = (\tau^1,\tau^2,\tau^3)$ are the three Pauli isospin matrices for nucleons.

meson	J^π	I	mass m[MeV]	$g^2/4\pi$ Bonn	GK
$\pi^\pm$	0^-	1	139.6	14.4	14.3
π^0			135.0		
η	0^-	0	548.8	4.95	0
ρ	1^-	1	770	0.48 (6.0)	0.55 (6.1)
ω	1^-	0	783	10.6	8.1 ± 1.5

table 1: Properties and coupling constants of mesons commonly used in Boson exchange models of the NN interaction. The Bonn [9] results refer to vertex functions modified by monopole form factors

$$F(q^2) = (\Lambda^2 - m^2)/(\Lambda^2 - q^2), \quad q^2 = q_o^2 - \vec{q}^2,$$

with λ = 1.5 GeV. Also shown are the coupling constants obtained by a dispersion theoretic analysis of Grein and Kroll (GK) [12]. For the vector mesons, the coupling constant $g_V^2/4\pi$ is given and the ratio g_T/g_V shown in parantheses (this ratio is small for the ω meson).

Fig. 2 shows a representative selection of nucleon-nucleon phase shifts in low and higher partial waves calculated with the recent one- and two-boson exchange interaction of the Bonn group [9]. This calculation includes a selected set not only of ($\pi\pi$) exchange, but also ($\pi\rho$), ($\pi\sigma$) and ($\pi\omega$) exchange processes. The results obtained with the Paris potential [7] are of similar quality.

Note that the higher partial waves up to laboratory energies $E_{lab} \simeq 100$ MeV are dominated by one-pion exchange, because of their peripheral nature.

+) We use conventions such that

$$\gamma_o = \begin{pmatrix} 1 & 0 \\ 0 & -1 \end{pmatrix}, \quad \vec{\gamma} = \begin{pmatrix} 0 & \vec{\sigma} \\ -\vec{\sigma} & 0 \end{pmatrix}, \quad \gamma_5 = \begin{pmatrix} 0 & 1 \\ 1 & 0 \end{pmatrix}, \quad \{\gamma_\mu,\gamma_\nu\} = 2g_{\mu\nu} \text{ with } g_{00} = 1,$$

$$g_{ij} = -\delta_{ij}; \quad \bar{\psi} = \psi^+\gamma_o$$

2.2 Reminder of the One-Pion Exchange interaction

The best known part of the nuclear force is one-pion exchange (OPE). It is the prototype of spin-isospin dependent interactions and plays a most important role in all subsequent discussions.

For a static, pointlike nucleon, the pion-nucleon interaction Hamiltonian derived from eq. (2.1a) by a non-relativistic reduction is

$$H_{\pi NN} = \frac{f}{m_\pi} \vec{\sigma}\cdot\vec{\nabla}\ \vec{\tau}\cdot\vec{\phi}(\vec{r}), \tag{2.2}$$

where $\vec{\sigma}$ and $\vec{\tau}$ are nucleon spin and isospin and $\vec{\phi}(\vec{r})$ is the isovector pionfield. Second order perturbation theory with $H_{\pi NN}$ gives the static one-pion exchange (OPE) potential (see Fig. 3). In momentum space

$$V_\pi(\vec{q}) = -\frac{f^2}{m_\pi^2}\frac{\vec{\sigma}_1\cdot\vec{q}\ \vec{\sigma}_2\cdot\vec{q}}{\vec{q}^2+m_\pi^2}\ \vec{\tau}_1\cdot\vec{\tau}_2\ , \tag{2.3}$$

where $\vec{q}$ is the momentum transfer carried by the exchanged pion. The coupling constant is

$$\frac{f}{m_\pi} = \frac{g_{\pi NN}}{2M}\ ,\quad \frac{g^2_{\pi NN}}{4\pi} \simeq 14 \qquad \text{(see table 1)} \tag{2.4}$$

where m_π and M are the pion and the nucleon mass, respectively, i.e. $f \simeq 1$. The V_π of eq. (2.3) can be split into a spin-spin and tensor piece,

$$V_\pi(\vec{q}) = -\frac{1}{3}\frac{f^2}{m_\pi^2}\left[\left(1-\frac{m_\pi^2}{q^2+m_\pi^2}\right)\vec{\sigma}_1\cdot\vec{\sigma}_2 + \frac{\vec{q}^2}{\vec{q}^2+m_\pi^2}S_{12}(\hat{q})\right]\vec{\tau}_1\cdot\vec{\tau}_2\ , \tag{2.5}$$

with

$$S_{12}(\hat{q}) = 3\,\vec{\sigma}_1\cdot\hat{q}\ \vec{\sigma}_2\cdot\hat{q} - \vec{\sigma}_1\cdot\vec{\sigma}_2\ , \tag{2.6}$$

where $\hat{q} = \vec{q}/|\vec{q}|$. In r-space, one obtains the familiar form:

$$\begin{aligned} V_\pi(\vec{r}) &= \frac{f^2}{m_\pi^2}\vec{\sigma}_1\cdot\vec{\nabla}\,\vec{\sigma}_2\cdot\vec{\nabla}\,\frac{e^{-m_\pi r}}{4\pi r}\ \vec{\tau}_1\cdot\vec{\tau}_2 \\ &= \frac{1}{3}\frac{f^2}{4\pi}\left\{\left[\frac{e^{-m_\pi r}}{r} - \frac{4\pi}{m_\pi^2}\delta^3(\vec{r})\right]\vec{\sigma}_1\cdot\vec{\sigma}_2 + \right. \\ &\quad \left.\left(1+\frac{3}{m_\pi r}+\frac{3}{m_\pi^2 r^2}\right)\frac{e^{-m_\pi r}}{r}S_{12}(\hat{r})\right\}\vec{\tau}_1\cdot\vec{\tau}_2\ . \end{aligned} \tag{2.7}$$

The characteristic feature of OPE is its strong tensor force. The δ-function piece is obviously an artifact of the assumed pointlike nature of the nucleon source. Nucleons are, of course, far from being pointlike objects, and we shall examine how their size and intrinsic structure modifies the properties of OPE at short distances.

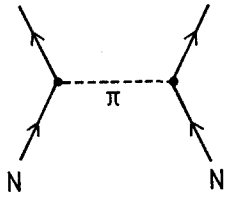

Figure 3: Static one-pion exchange interaction between nucleons

2.3 Isovector Two-Pion Exchange

At shorter distances, the spin-isospin dependent nucleon-nucleon interaction receives contributions from the exchange of two interacting pions in the channel with ($J^\pi = 1^-$, $I = 1$), the one carrying the quantum numbers of a ρ meson. (See Fig. 4)

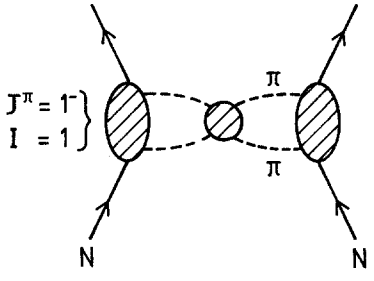

Figure 4: Exchange of a ($\pi\pi$) pair coupled to ($J^\pi = 1^-$, $I = 1$) including ρ exchange.

If the ($\pi\pi$) mass distribution is approximated by a single δ-function located at $m_\rho = 770$ MeV, and for infinitely heavy, pointlike nucleons, the ρ exchange interaction obtained by non-relativistic reduction from eq. (2.1b) becomes:

$$V_\rho(\vec{q}) = -\frac{f_\rho^2}{m_\rho^2}\,\frac{(\vec{\sigma}_1\times\vec{q})\cdot(\vec{\sigma}_2\times\vec{q})}{\vec{q}^{\,2}+m_\rho^2}\;\vec{\tau}_1\cdot\vec{\tau}_2\;. \tag{2.8}$$

We note that the $\vec{\sigma}$ x $\vec{q}$ type interaction comes from the dominant tensor coupling $\bar{\psi}\,\sigma_{\mu\nu}\,\psi\,\partial^\nu\rho^\mu$ of the ρ meson to the nucleon. Here $f_\rho/m_\rho = (g_T)_{\rho NN}/2M$. Empirically, one finds $f_\rho^2/m_\rho^2 \simeq 2\,f_\pi^2/m_\pi^2 \simeq 2m_\pi^{-2}$. In r-space,

$$V_\rho(\vec{r}) = \frac{1}{3}\frac{f_\rho^2}{4\pi}\left\{2\left[\frac{e^{-m_\rho r}}{r} - \frac{4\pi}{m_\rho^2}\,\delta^3(\vec{r})\right]\vec{\sigma}_1\cdot\vec{\sigma}_2 - \right.$$

$$\left. -\left(1+\frac{3}{m_\rho r}+\frac{3}{m_\rho^2 r^2}\right)\frac{e^{-m_\rho r}}{r}\,S_{12}(\hat{r})\right\}\vec{\tau}_1\cdot\vec{\tau}_2\;. \tag{2.9}$$

The ρ exchange tensor force has opposite sign as compared to π exchange and therefore tends to reduce the pathologically strong OPE tensor force at short distance. However,

a picture like this is probably only of limited relevance, since the ρ meson Compton wavelength m_ρ^{-1} is comparable to the nucleon size, as mentioned before. That is, one has to expect that V_ρ is cut down massively by form factors.

LECTURE 2

3. Pion-Nucleon Coupling in Relativistic Quark Models

Given the fact that nucleons have their own intrinsic quark structure, it is necessary to address the question why a description of nuclei in terms of nucleon quasi particles and mesons instead of quarks is successful even at momentum transfers where one would expect the size of nucleons to play a substantial role. There is, of course, no satisfactory answer to this question. It is nevertheless useful to obtain some insight into the relevant length scales involved in pion-nucleon interactions, and in particular to see how the magnitude of the phenomenological pion-nucleon coupling constant $g_{\pi NN}$ can be related to the underlying quark dynamics.

3.1 Facts from QCD

Non-strange hadrons are composed uf u- and d-quarks which form a flavour-SU(2) (isospin) doublet. In this flavour subsector, the QCD Lagrangian is

$$\mathcal{L}_{QCD} = \bar{q}(x)\left[i\gamma_\mu D^\mu - m\right]q(x) - \frac{1}{4} F^a_{\mu\nu}(x) F_a^{\mu\nu}(x), \qquad (3.1)$$

where q(x) are the quark fields and m is the mass matrix:

$$q(x) = \begin{pmatrix} q_u(x) \\ q_d(x) \end{pmatrix}, \quad m = \begin{pmatrix} m_u & 0 \\ 0 & m_d \end{pmatrix}. \qquad (3.2)$$

Here

$$D_\mu \equiv \partial_\mu - ig\frac{\lambda_a}{2} G^a_\mu(x), \qquad (3.3)$$

where $G^a_\mu(x)$ is the gluon field with color indices a = 1, ..., 8; $F^a_{\mu\nu}$ is the corresponding field tensor, and λ_a are the SU(3) color matrices.

Now, there are many hints that the (current) quark masses m_u and m_d are very small compared to typical hadron masses. The important point is that for $m_u = m_d = 0$, $\mathcal{L}_{QCD}$ of eq. (3.1) is invariant under the chiral transformation

$$q(x) \to e^{i\gamma_5 \vec{\tau}\cdot\vec{\theta}} q(x), \quad \bar{q}(x) \to \bar{q}(x)\, e^{i\gamma_5 \vec{\tau}\cdot\vec{\theta}}. \qquad (3.4)$$

That is, chiral symmetry is a fundamental symmetry of QCD with massless quarks. This symmetry combines the conservation of helicity for massless, free Fermions, with the (u,d) iso-doublet structure of the quark fields.

Invariance under the chiral transformation, eq. (3.4), implies that the quark axial current,

$$\vec{A}_\mu(x) = \bar{q}(x)\,\gamma_\mu\gamma_5\,\frac{\vec{\tau}}{2}\,q(x) \tag{3.5}$$

is conserved for free quarks, i.e.

$$\partial^\mu \vec{A}_\mu(x) = 0\,. \tag{3.6}$$

On the other hand, the solutions of the equations of motion derived from $\mathcal{L}_{QCD}$ are expected to generate confinement for individual quarks. Once confinement sets in, chiral symmetry is necessarily broken. To illustrate this, consider for example a single, massless quark whose motion is partly confined by a reflecting wall. Reflection at the wall implies that the quark momentum changes from $\vec{p}$ to $-\vec{p}$, whereas the quark spin remains unaffected. Thus the helicity $h = \vec{\sigma}\cdot\vec{p}/|\vec{p}|$ changes sign, i.e. the quark wavefunction is not an eigenfunction of helicity any more. In more general terms, chiral symmetry is spontaneously (or rather: dynamically) broken. This can be cast into simple phenomenological terms as shown in the following section.

3.2 Confining Potentials and Chiral Symmetry breaking

The phenomenology of confined quarks has been developed quite successfully in terms of Bag Models [13] and their extension to incorporate Chiral Symmetry [14-16]. We shall follow here a slightly different path, though with a similar physical picture in mind, by assuming that non-strange baryons are composed of massless u- and d-quarks confined by a scalar potential M(r) [17,18]. This potential is to be interpreted as the mean field experienced by individual quarks and generated by the confining forces which are probably due to non-perturbative gluon interactions. Soliton models [19,20] simulate these degrees of freedom in terms of a scalar soliton field $\sigma(r)$, so that the local quark mass becomes $M(r) = g\sigma(r)$, where g is a coupling constant. The quark Hamiltonian in such a picture is ($\vec{\alpha} = \gamma_0\vec{\gamma}$, $\beta = \gamma_0$):

$$H = \vec{\alpha}\cdot\vec{p} + \beta M(r)\,, \tag{3.7}$$

and the quark fields $q(x) = q(\vec{r},t)$ satisfy the Dirac equation

$$\left[i\gamma_\mu\partial^\mu - M(r)\right] q(\vec{r},t) = 0\,. \tag{3.8}$$

The confining potential M(r) should have some of the qualitative features suggested by QCD, assuming that M(r) represents a mean field primarily of gluonic origin: in the hadron center, M(r) should be small, so as to allow quarks to move freely, in accordance with asymptotic freedom. Towards the surface, M(r) should grow rapidly to yield confinement. Absolute confinement requires $M(r) \to \infty$ beyond some distance from the hadron center.

An ansatz for M(r) can be made as a power series in r, or simply by a single power law $M(r) = cr^n$. For such potentials and the Dirac equation eq. (3.8) a virial theorem can be derived [21]: The potential energy,

$$E_{pot} = \int d^3r \, \langle q^+ \gamma_0 M(r) q \rangle$$

is related to the total energy E in a given quark orbit by

$$E_{pot} = \frac{E}{n+1} . \tag{3.9}$$

For n = 3 the confining potential $M(r) = cr^3$ essentially replaces the volume part of the energy in the standard MIT bag model, where the energy per quark is

$$\frac{E(R)}{N} = \frac{x}{R} + \frac{4\pi}{3N} BR^3 . \tag{3.10}$$

The first term in eq. (3.10) is to be interpreted as the quark kinetic energy, with x = 2.04 for the lowest $s_{1/2}$ orbit. The condition dE/dR = 0 implies that the volume term, $(4\pi/3N)BR^3$, is 1/4 of the total energy, just as for the r^3-potential. The parameter c for n = 3 plays the role of an energy density, which we expect to be of the order of 1 GeV/fm^3.

Consider now the axial current of a single quark satisfying the Dirac equation, eq. (3.8) We take the divergence and find, using the Dirac equation:

$$\partial^\mu A_\mu^\lambda(x) = M(r) \, \bar{q}(x) i\gamma_5 \tau^\lambda q(x) . \tag{3.11}$$

This result tell us that the breaking of chiral symmetry, measured by the nonzero divergence of the axial current, is directly related to the confining potential. The limit of free, massless quarks would be obtained with $M(r) \equiv 0$. The right hand side of eq. (3.11) acts as a pseudoscalar-isovector source function. This source function obviously peaks at the baryon surface, since M(r) rises like a power, whereas the quark wave functions q(r) decrease exponentially beyond a distance comparable to the baryon size.

3.3 Introducing the Goldstone Pion

If QCD has an underlying SU(2) x SU(2) chiral symmetry, then the dynamical breaking of this symmetry by confinement at the quark level must be restored by a compensating field carrying the quantum numbers of a pion. The Goldstone theorem requires the existence of such a Boson field with zero mass. To demonstrate this, one generalizes the axial current,

$$A_\mu^\lambda(x) = \bar{q}(x) \gamma_\mu \gamma_5 \frac{\tau^\lambda}{2} q(x) - f_\pi \partial_\mu \phi^\lambda(x) \quad + \text{terms non-linear in } \phi^\lambda \tag{3.12}$$

by introducing the pseudoscalar-isovector field $\phi^\lambda(x)$ just mentioned. Here f_π is a constant. Restoring chiral symmetry means to require that the divergence of eq. (3.12) vanishes.

Suppose now that we can omit the terms non-linear in ϕ^λ as a first approximation [16].

Then together with eq. (3.11), the condition $\partial^\mu A^\lambda_\mu = 0$ implies the following field equation for ϕ^λ:

$$f_\pi \Box \phi^\lambda(x) = M(r)\, \bar{q}(x)\, i\gamma_5 \tau^\lambda q(x). \tag{3.13}$$

The suggestion is, of course, to identify ϕ^λ with the pion. This pion has zero mass according to eq. (3.13). We refer to it as the Goldstone Boson associated with the breaking of chiral symmetry at the quark level.

The step from a conserved axial current to PCAC can be made by introducing a finite pion mass, $m_\pi = 140$ MeV. Furthermore, f_π should be identified with the pion decay constant, $f_\pi = 93$ MeV, since the pionic part of the axial current determines the decay rate for $\pi \to \mu\nu$. Eq. (3.13) is then replaced by

$$(\Box + m_\pi^2)\, \phi^\lambda(x) = \frac{M(r)}{f_\pi}\, \bar{q}(x)\, i\gamma_5 \tau^\lambda q(x), \tag{3.14}$$

and the divergence of the axial current becomes

$$\partial^\mu A^\lambda_\mu(x) = m_\pi^2 f_\pi \phi^\lambda(x). \tag{3.15}$$

In chiral bag models, the source function on the right hand side of eq. (3.14) is proportional to a δ-function at the bag boundary.

The pion is introduced here on purely phenomenological grounds, as in chiral bag models. There is no obvious relation to the pion as a bound $q\bar{q}$ pair at this level. A more profound approach can be based on the Nambu and Jona-Lasinio model [22]. This model starts from a chiral invariant effective Lagrangian for massless quarks and demonstrates that if the quarks acquire a non-zero effective mass by sufficiently strong self-interactions, at which point chiral symmetry is spontaneously broken, a bound quark-antiquark mode carrying pion quantum numbers develops with zero mass. The physical pion mass is then obtained by starting from finite, but small quark masses of order 10 MeV. The pion in such a picture is a coherent superposition of $q\bar{q}$ states [23] and has properties analogous to low-lying collective particle-hole states in many body systems. The pion core must be small ($r_\pi \lesssim 0.4$ fm) in order to obtain the correct decay constant f_π [24,25].

The very special nature of the pion as compared to other mesons is clearly one of the most fundamental aspects of nuclear forces, although we cannot go into further details here. Some interesting features of pion-nucleon dynamics can however be discussed already at the present level.

3.4 Pion-Nucleon Coupling and the Axial Form Factor

Suppose that nucleons are described by three massless [+] quarks occupying the lowest orbit of the confining potential M(r). Eq. (3.13) tells that the coupling of a pion to quarks in the nucleon is given by the source function

$$J_5^\lambda(x) = \frac{M(r)}{f_\pi} \sum_{j=1}^{3} \bar{q}_j(x)\, i\gamma_5 \tau^\lambda q_j(x). \tag{3.16}$$

In the static limit, we define a pion-nucleon form factor $G_{\pi NN}(q^2)$ by

$$-i\, G_{\pi NN}(q^2) \langle \vec{\sigma}\cdot\vec{q}\,\tau^\lambda \rangle = 2M \langle N | \int d^3r\, e^{i\vec{q}\cdot\vec{r}} J_5^\lambda | N \rangle, \tag{3.17}$$

where $\langle \vec{\sigma}\tau^\lambda \rangle$ refers to matrix elements taken with nucleon spin and isospin operators, and $|N\rangle$ is the SU(4) three-quark wave function of the nucleon. The πN coupling constant is

$$g_{\pi NN} = G_{\pi NN}(q^2=0). \tag{3.18}$$

(It is actually defined as $G_{\pi NN}(q^2 = m_\pi^2)$, but we ignore this minor detail.)

Another form factor of interest is the one related to the quark axial current. The axial form factor measures the spin distribution of quarks inside the nucleon . At momentum transfers $q^2 << 4M^2$, it is given by

$$G_A(q^2) \langle \sigma^i \tau^\lambda/2 \rangle = \langle N | \int d^3r\, e^{i\vec{q}\cdot\vec{r}} A_i^\lambda(\vec{r}) | N \rangle, \tag{3.19}$$

where A_i^λ is one of the three-vector components (i = 1,2,3) of the $A_\mu^\lambda = \bar{q}\,\gamma_\mu\gamma_5(\tau^\lambda/2)q$, summed over the three valence quarks. The $G_A(q^2)$ is normalized according to

$$g_A = G_A(q^2=0), \tag{3.20}$$

where g_A is the axial charge. (Empirically, g_A = 1.26). Now, it can be shown [25,26] that $G_A(q^2)$ does not receive contributions from a pionic term proportional to $f_\pi \partial_\mu \phi$ of the axial current as long as ϕ is a continuous function. This makes $G_A(q^2)$ a particularly suitable quantity to discuss the quark core size. For a confining potential $M(r) = cr^3$ with $c \simeq 1$ GeV/fm^3, we find the result, Fig. 5. The axial charge comes out to be g_A = 1.21. Center-of-mass corrections, obtained by projection of the quark momenta onto good total momentum, turn out to be small, if the projection procedure is constrained by the gauge invariance requirement for the corresponding electromagnetic current [26]. The rms radius associated with $G_A(q^2)$ is $\langle r^2 \rangle^{1/2} \simeq 0.6$ fm.

It is straightforward to show by using the Dirac equation that $g_{\pi NN}$ and g_A are connected by the Goldberger-Treiman relation,

---

+) We could add at this point small current quark masses of about 10 MeV, consistent with a finite, but small pion mass.

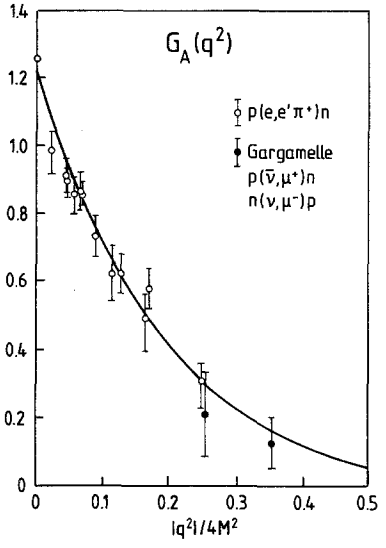

Figure 5: The nucleon axial form factor calculated for three quarks confined in the potential $M(r) = cr^3$ with $c = 0.95$ GeV/fm^3 [26].

$$g_{\pi NN} = \frac{M}{f_\pi} g_A \,. \tag{3.21}$$

For $g_A = 1.21$ obtained with the cr^3 potential, $g_{\pi NN} \simeq 12$ results, to be compared with the empirical value $g_{\pi NN} \simeq 13$.

The pion-nucleon source function is shown in Fig. 6. It exhibits the characteristic surface peaking. The resulting form factor $G_{\pi NN}(q^2)$ [26] is slightly softer than the axial form factor $G_A(q^2)$. Similar conclusions have been drawn in ref. [25].

Unlike the nucleon electromagnetic form factors, $G_A(q^2)$ receives practically no contribution from the pion cloud in this model. Effects from 3π states could be present in principle, but they would probably change the picture very little, the dominant contribution in this channel being the A_1 with a mass of no less than 1.3 GeV.

In chiral quark models, the difference in radius between the axial form factor, which measures essentially the spin distribution within the nucleon, and the charge radius $\langle r_c^2 \rangle^{1/2} = 0.83$ fm is assigned to the charged pion cloud surrounding the quark core. We present in Fig. 7 the results of such a calculation [17] where the quark core is the same as used to obtain $G_A(q^2)$ of Fig. 5. The calculation includes approximate center-of-mass corrections. It shows that the proton charge radius is in fact determined largely by the pion cloud which represents about 1/3 of the total charge.

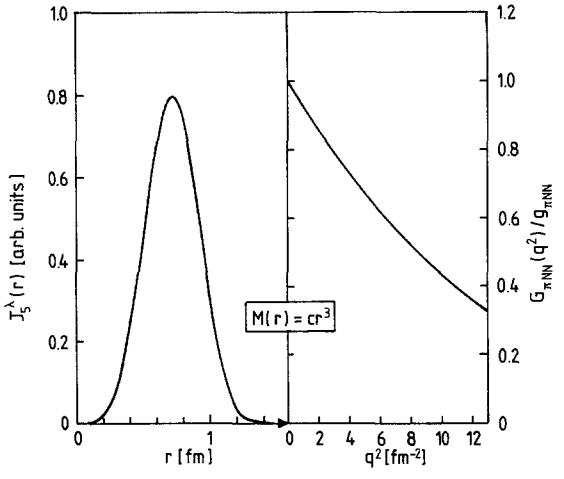

Figure 6: Pion-nucleon source function $\langle N|J_5^\lambda(r)|N\rangle$ (left) and the corresponding pion-nucleon form factor $G_{\pi NN}(q^2)$ evaluated according to eqs.(3.16,17) with a confining potential $M(r) = cr^3$ with $c = 0.95$ GeV/fm^3.

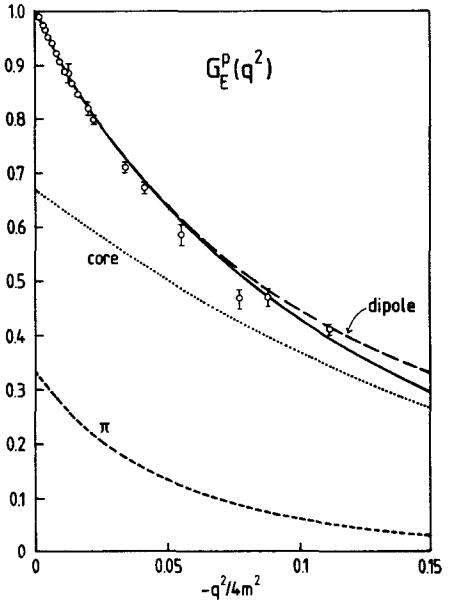

Figure 7: Proton charge form factor calculated according to ref. [27]. The contribution of the quark core and of the pion cloud are shown separately; the sum of both is compared to data. The quark core is the same as the one giving the $G_A(q^2)$ of Fig. 5.

3.5 Constraints on the OPE Tensor Force: the deuteron asymptotic D/S-ratio

A quark core of about 1/2 fm radius will introduce substantial modifications as compared to OPE with pointlike nucleon sources. The static OPE potential with form factors becomes

$$V_\pi(\vec{q}) = -\frac{G^2_{\pi NN}(q^2)}{4M^2}\,\frac{\vec{\sigma}_1\cdot\vec{q}\;\vec{\sigma}_2\cdot\vec{q}}{\vec{q}^2+m_\pi^2}\;\vec{\tau}_1\cdot\vec{\tau}_2\;. \qquad (3.22)$$

For $G_{\pi NN}(q^2)$ as obtained from a quark core following the preceeding discussion, we show the resulting tensor potential in Fig. 8, for a core radius $\langle r^2\rangle^{1/2}$ = 0.5 fm. The finite size of the core effectively weakens the tensor force, by an amount determined by the rms radius.

One of the best possibilities to examine the tensor force is by investigating the asymptotic D/S-ratio in the deuteron. We follow here the discussion of ref. [28]. The D/S-ratio η is defined in terms of the asymptotic S- and D-state components of the deuteron wave function (u(r) and w(r), respectively) as follows:

$$u(r) \xrightarrow[r\to\infty]{} N e^{-\alpha r}\,,\quad w(r) \xrightarrow[r\to\infty]{} \eta N\left(1+\frac{3}{\alpha r}+\frac{3}{\alpha^2 r^2}\right)e^{-\alpha r}\,, \qquad (3.23)$$

where $\alpha^2 = \varepsilon M$ and ε is the deuteron binding energy. The value of η is determined to such high accuracy that it allows for a detailed test of the tensor potential at

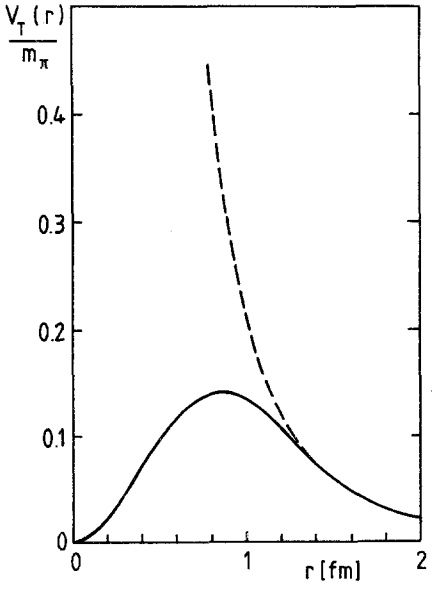

Figure 8: The one-pion exchange tensor potential with point-like nucleons (dashed curve) and modified by form factors $G_{\pi NN}(q^2)$ calculated with a quark confining potential M(r) = cr^3, c = 1 GeV/fm^3 (solid curve).

distances $r \gtrsim 0.6$ fm, the unknown short distance behaviour being suppressed [28].

We show in Fig. 9 a calculation of η following the method of Ericson and Rosa-Clot, using the quark core πN form factor $G_{\pi NN}(q^2)$ as input, and varying the quark core density radius $\langle r^2 \rangle^{1/2}$. The result indicates that the measured value of η sets an upper limit to $\langle r^2 \rangle^{1/2}$ of about 0.6 fm. This result does not depend on the precise form of $G_{\pi NN}(q^2)$, the essential parameter being just $\langle r^2 \rangle$ [29]. It may well be, of course, that $G_{\pi NN}(q^2)$ in such an analysis represents a variety of complicated short-distance processes, so that the immediate relation to the quark core size is obscured. In any case, the data tell that deviations from pointlike OPE should effectively not extend beyond a distance $r \gtrsim 0.6$ fm.

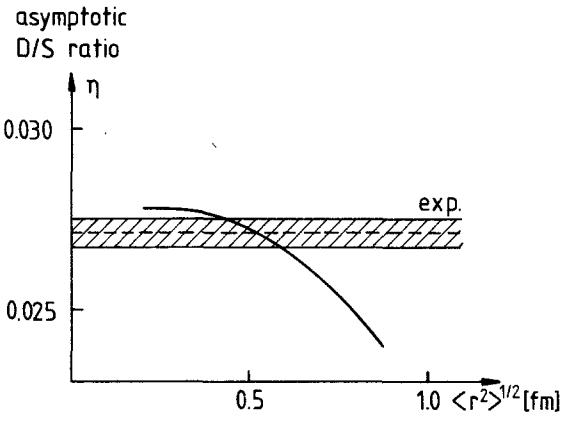

Figure 9: Deuteron asymptotic D/S-ratio calculated according as in [28], with $G_{\pi NN}(q^2)$ from eq. (3.17). The radius $\langle r^2 \rangle^{1/2}$ refers to the density distribution of the quark core as calculated with confining potential $M(r) = cr^3$ (see text).

3.6 Nucleonic Spin-Isospin Transitions, the Δ(1232), and πNΔ -Coupling

Three u or d quarks in a $(1s_{1/2})^3$ configuration of a bag or confining potential can be coupled either to a spin 1/2, isospin 1/2 state (the nucleon) or a spin 3/2, isospin 3/2 state (the Δ). The mass splitting between N(938) and Δ(1232) is due to spin-dependent residual forces. The most important mechanisms contributing to this splitting are supposed to be chromomagnetic interactions from gluon exchange and the spin-isospin dependent self-interactions of the nucleon or Δ via the surrounding pion cloud (see e.g. refs. [15,16]).

Such a model, together with the pion-quark interaction developed before, necessarily implies a strong πNΔ coupling. The reason is that the transition from nucleon to Δ(1232) is made by a single spin-isospin flip on one of the quarks, without changing their spatial $(1s)^3$ configuration.

Given the pion-quark source function J_5^λ of eq. (3.16), we can define a πNΔ transition

form factor $G_{\pi N\Delta}(q^2)$ by

$$-i\, G_{\pi N\Delta}(q^2)\, \langle \vec{S}^+ \cdot \vec{q}\, T^+_\lambda \rangle = 2\sqrt{M M_\Delta}\, \langle \Delta | \int d^3r\, e^{i\vec{q}\cdot\vec{r}}\, J^\lambda_5 | N \rangle, \quad (3.24)$$

where $|N\rangle$ and $|\Delta\rangle$ are the quark model wave functions of nucleon and $\Delta(1232)$, respectively, and the matrix element $\langle \vec{S}^+ \vec{T}^+ \rangle$ on the left hand side refers to transition matrix elements taken between spin-isospin - 1/2 and spin-isospin - 3/2 states. The transition operators are defined as

$$\begin{aligned} \langle 3/2\, m_\Delta | S^+_\mu | 1/2\, m_N \rangle &= (3/2\, m_\Delta | 1\mu\, 1/2\, m_N), \\ \langle 3/2\, \tau_\Delta | T^+_\mu | 1/2\, \tau_N \rangle &= (3/2\, \tau_\Delta | 1\mu\, 1/2\, \tau_N) \end{aligned} \quad (3.25)$$

A property of the spin transition operators which will be used frequently in practical applications is

$$S_i S^+_j = \delta_{ij} - \tfrac{1}{3}\sigma_i \sigma_j, \quad (3.25a)$$

where i and j denote Cartesian components (i = 1,2,3). Since the orbital parts of the three-quark-wave functions $|N\rangle$ and $|\Delta\rangle$ are the same as long as the N-Δ mass splitting is treated in first order perturbation theory, the ratio of $G_{\pi N\Delta}$ and $G_{\pi NN}$ is determined entirely by spin-isospin coupling coefficients, i.e. by the underlying SU(2) x SU(2) symmetry of the problem. More precisely [30]:

$$\frac{\langle \Delta | J^\lambda_5 | N \rangle}{\langle N | J^\lambda_5 | N \rangle} = \sqrt{\frac{72}{25}}\,. \quad (3.26)$$

The resulting model of πNN and $\pi N\Delta$ couplings can be summarized in terms of the interaction Hamiltonians

$$H_{\pi NN} = i\, \frac{f(q^2)}{m_\pi}\, \vec{\sigma}\cdot\vec{q}\; \vec{\tau}\cdot\vec{\phi}\,, \quad (3.27)$$

$$H_{\pi N\Delta} = i\, \frac{f_\Delta(q^2)}{m_\pi}\, \vec{S}^+\cdot\vec{q}\; \vec{T}^+\cdot\vec{\phi} + h.c.\,, \quad (3.28)$$

where

$$\begin{aligned} f(q^2) &= \frac{m_\pi}{2M}\, G_{\pi NN}(q^2)\,, \\ f_\Delta(q^2) &= \frac{m_\pi}{2\sqrt{M M_\Delta}}\, G_{\pi N\Delta}(q^2)\,, \end{aligned} \quad (3.29)$$

with $f(q^2 = 0) \equiv f = 1$, $f^2_\Delta/f^2 = 72/25$. This gives already a reasonable description of p-wave pion-nucleon scattering and one-pion exchange forces. More detailed quantitative agreement can be obtained by adding relativistic corrections and readjusting f_Δ to the Chew-Low value, $f_\Delta = 2$ [5], the model we shall adopt in many-body applications.

3.7 Summary

Chiral symmetry is a fundamental symmetry of QCD with massless u and d quarks. Confinement necessarily breaks chiral symmetry at the quark level and implies the existence of a massless Goldstone pion. The finite pion mass is probably related to finite, but small current quark masses m_u, m_d of order 10 MeV. Chiral bag or confinement potential models are a convenient way to introduce the coupling of pions to quarks at the baryon surface. In such models, the πNN or $\pi N\Delta$ form factor can be calculated; for a cr^3 confining potential it turns out to be well approximated by

$$f(q^2) = \sqrt{\frac{25}{72}}\, f_\Delta(q^2) = f \exp\left[-\frac{\vec{q}^2}{\Lambda^2}\right], \tag{3.30}$$

where Λ^{-1} is related to the quark core rms radius. For example, one obtains Λ = 750 MeV for $\langle r^2\rangle^{1/2}$ = 0.5 fm. Such relatively soft pion-nucleon form factors are consistent with the nucleon axial form factor (although the experimental uncertainties are unfortunately too large at present to draw more quantitative conclusions). It would be difficult, however, to accomodate such a Λ with the existing one-boson exchange phenomenology of the nucleon-nucleon interaction [10] which suggests cutoffs Λ of about 1 GeV or larger. To establish connections between boson exchange models and the underlying quark dynamics at short distance remains as a key problem.

LECTURE 3

4. Virtual Pions in Nuclei

4.1 Pion Exchange Currents

Some of the strongest evidence for pionic degrees of freedom in nuclei comes from investigations with electromagnetic probes. The exchange of virtual charged pions between nucleons contributes genuine two-body pieces to the total nuclear current. Effects of these socalled exchange currents have been studied in great detail [31,32], especially for simple systems like the deuteron.

We recall that the static pion-nucleon interaction Hamiltonian (with pointlike nucleons) is

$$H_{\pi NN} = \frac{f}{m_\pi}\,(\vec{\sigma}\cdot\vec{\nabla})(\vec{\tau}\cdot\vec{\phi}). \tag{4.1}$$

Now, the rule for introducing the photon field in a gauge invariant way is to replace

$$\vec{\nabla} \rightarrow \vec{\nabla} \mp ie\vec{A}, \tag{4.2}$$

where $\vec{A}$ is the vector potential, and $\pm$ refers to a π^+ or π^- meson, respectively. This generates an interaction of the form

$$H_{\gamma\pi N} = \frac{f}{m_\pi} ie\sqrt{2}\ \tau_\pm \phi_\mp \vec{\sigma}\cdot\vec{A}. \tag{4.3}$$

Furthermore, the pion itself carries a current

$$\vec{J}_\pi = ie\left[\phi_+ \vec{\nabla}\phi_- - \phi_- \vec{\nabla}\phi_+\right], \tag{4.4}$$

which interacts with the photon, the corresponding term of the interaction being

$$H_{\gamma\pi} = \vec{J}_\pi \cdot \vec{A}. \tag{4.5}$$

To lowest order in the two-body one-pion exchange interaction, perturbation theory with $H_{int} = H_{\pi NN} + H_{\gamma\pi N} + H_{\gamma\pi}$ generates the Feynman diagrams shown in Fig. 10.

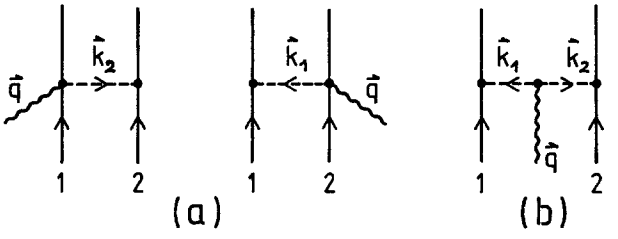

Figure 10: Two-body exchange currents from OPE, (a) Pair current; (b) pionic current.

The two diagrams (a) contain the point interaction $H_{\gamma\pi N}$ together with $H_{\pi N}$, connected by the propagator of the exchanged pion. This part is called the pair current because it derives a non-relativistic reduction of a process which relativistically (with γ_5 coupling) involves the virtual excitation of a particle-antiparticle pair. The corresponding two-nucleon current is

$$\vec{J}_{pair}(\vec{k}_1,\vec{k}_2) = -ie\left(\frac{f^2}{m_\pi^2}\right)\left[\vec{\tau}(1)\times\vec{\tau}(2)\right]_3 \left\{\frac{\vec{\sigma}_1(\vec{\sigma}_2\cdot\vec{k}_2)}{\vec{k}_2^{\,2}+m_\pi^2} - \frac{\vec{\sigma}_2(\vec{\sigma}_1\cdot\vec{k}_1)}{\vec{k}_1^{\,2}+m_\pi^2}\right\}. \tag{4.6}$$

The isospin dependence reflects the fact that the nucleon isospins always come in the combination $\tau_-(1)\tau_+(2) - \tau_+(1)\tau_-(2) = 2i\,[\vec{\tau}(1)\times\vec{\tau}(2)]_3$.

The term Fig. 10b represents the coupling of the photon to the exchanged pion. The pion current, eq. (4.4), gives a factor $(\vec{k}_1 - \vec{k}_2)$. The πNN vertex $H_{\pi NN}$ appears twice. There are two pion propagators, one for each pion of momentum $\vec{k}_1$ and $\vec{k}_2$, respectively

$$\vec{J}_\pi(\vec{k}_1,\vec{k}_2) = ie\left(\frac{f^2}{m_\pi^2}\right)[\vec{\tau}(1)\times\vec{\tau}(2)]_3 \frac{\vec{\sigma}_1\cdot\vec{k}_1\,(\vec{k}_1-\vec{k}_2)\,\vec{\sigma}_2\cdot\vec{k}_2}{(\vec{k}_1^2+m_\pi^2)(\vec{k}_2^2+m_\pi^2)} \,. \tag{4.7}$$

Note that the sum of pionic and pair current, if multiplied by $\vec{q} = \vec{k}_1 + \vec{k}_2$, becomes

$$\vec{q}\cdot(\vec{J}_{pair} + \vec{J}_\pi) =$$

$$= -ie\left(\frac{f^2}{m_\pi^2}\right)[\vec{\tau}(1)\times\vec{\tau}(2)]_3 \left\{\frac{\vec{\sigma}_1\cdot\vec{k}_1\;\vec{\sigma}_2\cdot\vec{k}_1}{\vec{k}_1^2+m_\pi^2} - \frac{\vec{\sigma}_1\cdot\vec{k}_2\;\vec{\sigma}_2\cdot\vec{k}_2}{\vec{k}_2^2+m_\pi^2}\right\} \tag{4.8}$$

This demonstrates that the pionic and pair currents have always to be taken together in order to satisfy current conservation (or equivalently, gauge invariance).

It is useful also to present the currents in r-space

$$\vec{J}(\vec{x},\vec{r}_1,\vec{r}_2) = \int \frac{d^3k_1}{(2\pi)^3}\,\frac{d^3k_2}{(2\pi)^3}\; e^{i\vec{k}_1\cdot(\vec{r}_1-\vec{x})}\; e^{i\vec{k}_2\cdot(\vec{r}_2-\vec{x})}\,\vec{J}(\vec{k}_1,\vec{k}_2)\,. \tag{4.9}$$

This yields

$$\vec{J}_{pair}(\vec{x},\vec{r}_1,\vec{r}_2) = -e\left(\frac{f^2}{4\pi}\right)[\vec{\tau}(1)\times\vec{\tau}(2)]_3\; Y_1(m_\pi r)\cdot$$

$$\left[\vec{\sigma}_1\,(\vec{\sigma}_2\cdot\hat{r})\,\delta^3(\vec{r}_1-\vec{x}) + \vec{\sigma}_2\,(\vec{\sigma}_2\cdot\hat{r})\,\delta^3(\vec{r}_2-\vec{x})\right]\,; \tag{4.10a}$$

$$\vec{J}_\pi(\vec{x},\vec{r}_1,\vec{r}_2) = -e\left(\frac{f^2}{4\pi}\right)[\vec{\tau}(1)\times\vec{\tau}(2)]_3\;\cdot$$

$$(\vec{\nabla}_1-\vec{\nabla}_2)\,(\vec{\sigma}_1\cdot\vec{\nabla}_1)(\vec{\sigma}_2\cdot\vec{\nabla}_2)\; Y_0(m_\pi|\vec{x}_1-\vec{x}|)\,Y_0(m_\pi|\vec{r}_2-\vec{x}|)\,. \tag{4.10b}$$

This illustrates most clearly the way in which the photon couples to the charged pion at the point $\vec{x}$ between the two nucleons located at points $\vec{r}_1$ and $\vec{r}_2$. Here $Y_0(z) = \frac{e^{-z}}{z}$ and $Y_1(z) = (1+\frac{1}{z})\,Y_0(z)$.

The above expressions are obtained for pointlike nucleons and pions. At high momentum transfers, modifications due to the finite size of nucleons and pions should be introduced. This is not a trivial procedure since the introduction of form factors has to be done such that gauge invariance is strictly satisfied.

4.2 The Exchange Magnetic Moment

Pion exchange currents have substantial influence on magnetic properties of nuclei in general, and on magnetic moments in particular. We recall that the magnetic moment density is related to the total current $\vec{J}$ by

$$\vec{\mu}(\vec{x}) = \tfrac{1}{2}\,\vec{x}\times\vec{J}(\vec{x})\,, \tag{4.11}$$

where $\vec{J}$ contains both single-nucleon currents and two-body exchange currents,

$$\vec{J}(\vec{x}) = \sum_{i=1}^{A} \vec{J}_i(\vec{x}) + \vec{J}_{ex}(\vec{x}). \tag{4.12}$$

The exchange magnetic moment is given by

$$\vec{\mu}_{ex} = \frac{1}{2}\int d^3x \left[\vec{x} \times \vec{J}_{ex}(\vec{x})\right]. \tag{4.13}$$

By far the dominant contribution comes from the pair current. Using eq. (4.10a) one obtains

$$\vec{\mu}_{ex}(1,2) = \frac{ef^2}{8\pi}\left[\vec{\tau}(1)\times\vec{\tau}(2)\right]_3 \cdot$$
$$\cdot\left\{\left[\vec{\sigma}_1\times\vec{r}_1\right](\vec{\sigma}_2\cdot\hat{r}) + (\vec{\sigma}_1\cdot\hat{r})\left[\vec{\sigma}_2\times\vec{r}_2\right]\right\} Y_1(m_\pi r), \tag{4.14}$$

where $\vec{r} = \vec{r}_1 - \vec{r}_2$. The exchange magnetic moment gives a characteristic correction to g_ℓ, the orbital g-factor of a nucleon in a nucleus. For example, an odd proton can exchange a π^+ with neutrons in the core. The corresponding correction $\delta g_\ell(p)$ is positive Similarly, if the odd particle is a neutron, the corresponding $\delta g_\ell(n)$ arises from a π^- exchanged with protons in the core. Hence $\delta g_\ell(n)$ is negative, and these considerations lead to

$$\frac{\delta g_\ell(p)}{\delta g_\ell(n)} = -\frac{N}{Z} \tag{4.15}$$

for pion exchange corrections to g_ℓ. The above arguments are summarized in the form [33]:

$$\delta g_\ell = \zeta \tau_3, \tag{4.16}$$

where actual calculations yield $\zeta = 0.1 - 0.2$. The isovector character of δg_ℓ is of course related to the isovector nature of the pionic current. The δg_ℓ due to pion exchange effects is a substantial fraction of the measured δg_ℓ in various nuclei (see T. Yamazaki in ref. [33]), but a detailed discussion of higher order configuration mixing effects is necessary to make the discussion quantitative.

4.3 The Δ(1232) Exchange Current

The Δ(1232) is reached from the nucleon by a spin-flip isovector transition which can be induced either by a pion or by the isovector M1 part of a photon field. The γNΔ coupling is of the type

$$H_{\gamma N\Delta} = i\frac{f_{\gamma N\Delta}}{m_\pi}\left(\vec{S}^+\times\vec{q}\right)\cdot\vec{A}\, T_3^+, \tag{4.17}$$

where $\vec{A}$ is the electromagnetic vector potential and $\vec{S}^+$, $\vec{T}^+$ refer to the (1/2 → 3/2) spin and isospin transition operators, eq. (3.25). The coupling strength can be determined from the photoproduction of neutral pions ($\gamma N \to \pi^0 N$) which is strongly dominated by the M1 excitation of the Δ(1232) via eq. (4.17). One obtains $f_{\gamma N\Delta} = 0.116$ and notices

that the following ratio holds to good accuracy:

$$\frac{f_{\gamma N\Delta}}{f_{\pi N\Delta}} = \frac{e}{g_{\pi NN}}\,\mu_v \tag{4.18}$$

where $g^2_{\pi NN}/4\pi = 14.4$ and μ_v is the isovector magnetic moment of the nucleon,

$$\mu_v = \tfrac{1}{2}(\mu_p - \mu_n),$$

with $\mu_p = 2.79$ and $\mu_n = -1.91$. Eq. (4.18) represents the ratio of electromagnetic to strong interaction scales, the additional μ_v arising because of the isovector magnetic dipole nature of the transition.

The virtual excitation of a $\Delta(1232)$ followed by pion exchange contributes to the two-body exchange current, as shown in Fig. 11. Following standard rules, one obtains for this part of the current:

$$\vec{J}_\Delta(\vec{q},\vec{k}_1,\vec{k}_2) = ie\,\frac{4}{9}\,\frac{f\,f_{\pi N\Delta}\,f_{\gamma N\Delta}}{m_\pi^3\,(M_\Delta - M)}\cdot$$

$$\cdot\Big\{\Big[4\tau_3(1)\,\frac{\vec{\sigma}_1\cdot\vec{k}_1\,(\vec{k}_1\times\vec{q})}{\vec{k}_1^{\,2}+m_\pi^2} + (1\leftrightarrow 2) -$$

$$-\,[\vec{\tau}(1)\times\vec{\tau}(2)]_3\Big[\frac{(\vec{\sigma}_1\times\vec{k}_1)\,\vec{\sigma}_2\cdot\vec{k}_2}{\vec{k}_2^{\,2}+m_\pi^2} - (1\leftrightarrow 2)\Big]\times\vec{q}\Big\}. \tag{4.19}$$

The ΔN mass difference $M_\Delta - M$ appearing in the denominator corresponds to virtual Δ-excitation after photon absorption. The reverse ordering is also possible as shown in Fig. 11, but involves the energy denominator in the form $(M_\Delta + M)^{-1}$ and is therefore suppressed. The interpretation of the isospin structure of the different terms in eq. (4.19) is straightforward. The first two terms which do not change the charge of either nucleon 1 or nucleon 2 correspond to the exchange of a π^0. The other terms proportional to $[\vec{\tau}(1) \times \vec{\tau}(2)]_3$ represent the exchange of charged ($\pi^\pm$) pions.

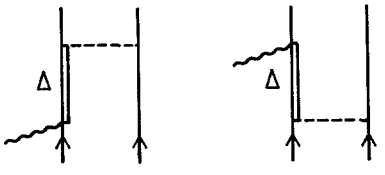

Figure 11: Exchange current involving the virtual excitation of a $\Delta(1232)$.

4.4. Exchange Currents in Few-Nucleon Systems

4.4.1 Deuteron Electrodisintegration

A classical example of evidence for pion exchange currents is the backward inelastic electron-deuteron scattering process

$$e + d \rightarrow e' + p + n$$

near threshold. The basic process is the same as in the $np \rightarrow d\gamma$ reaction at threshold, but now taken at high momentum transfers. There the only possibility for the final pn pair is to be in a $^1S_0$ state which is then reached from the $^3S_1 - {}^3D_1$ deuteron ground state by an M1 transition.

In the one-photon approximation close to threshold, the double differential cross section at large momentum transfers is given by

$$\frac{d^2\sigma}{dE'd\Omega} = C(\theta,E)\left\{\hat{k}'\cdot\vec{J}_{fi}^{\,*}\,\hat{k}\cdot\vec{J}_{fi} + \hat{k}\cdot\vec{J}_{fi}^{\,*}\,\hat{k}'\cdot\vec{J}_{fi} + 2\,|\vec{J}_{fi}|^2 \sin^2\frac{\theta}{2}\right\}, \qquad (4.20)$$

where $C(\theta,E)$ contains the Mott cross section and kinematic factors, and $(E,\vec{k})$, $(E',\vec{k}')$ are the in- and outgoing electron four-momenta.

The matrix elements $\vec{J}_{fi}$ receive contributions from one-body (impulse approximation) and two-body (exchange) currents. The one-body transition form factor has a characteristic minimum at $q^2 \simeq 12$ fm^{-2} due to interference between $^3D - {}^1S$ and $^3S - {}^1S$ transitions. The matrix elements due to different parts of the current operator are shown in Fig. 12, taken from ref. [34]. We note that the pair current $\vec{J}_{pair}$ dominates at large momentum transfers, with negligible additional effects from the pionic current $\vec{J}_\pi$; the $\Delta(1232)$ current $\vec{J}_\Delta$ also contributes, but much less than the pair current.

The comparison with data taken at Saclay [35] is shown in Fig. 12, where pionic exchange currents are incorporated following ref. [36]. Similar results have been obtained in ref. [37].

The agreement of the theory with data at relatively low q^2 is essentially a consequence of chiral symmetry and soft pion theorems which are implicit in the $q^2 \rightarrow 0$ limit of the exchange current. The interesting feature is the validity of this simplest possible description of exchange currents exclusively in terms of pions even at large momentum transfers. It seems then that the short range nuclear forces suppress short distance corrections to this picture rather efficiently.

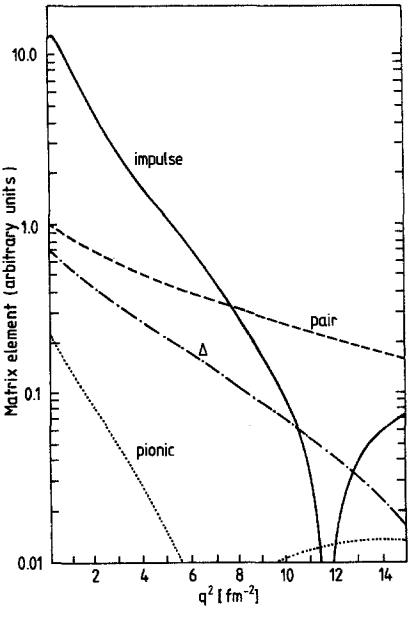

Figure 12: Contributions to the deuteron electrodisintegration matrix element [34] from pair, pionic and Δ(1232) exchange currents as compared to the impulse approximation.

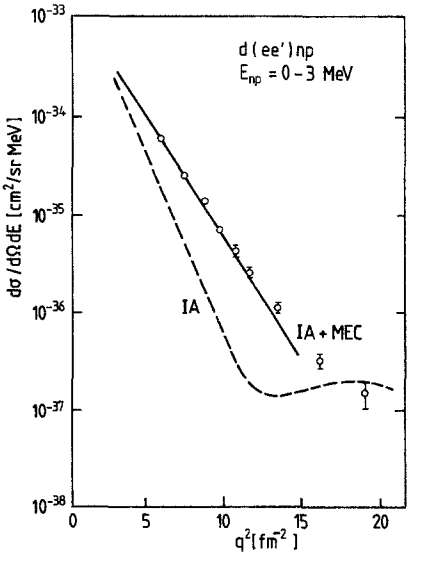

Figure 13: Differential cross section for d(e,e')np close to threshold. Dashed curve: impulse approximation; solid curve: inclusion of pair current; calculations: [36,37]; data from [35].

4.4.2 The ^{3}He Magnetic Form Factor

Another example of the influence of mesonic exchange currents is the magnetic form factor of ^{3}He. From our previous discussion, one naturally expects that the dominant M1 structure of the pair current should show up most pronouncedly in magnetic observables. This is demonstrated here for the form factor related to the spin distribution of nucleons in ^{3}He, measured by high resolution elastic electron scattering at backward angles.

This form factor is related to the magnetic moment density $\vec{\mu}(\vec{x})$ of eqs. (4.11, 4.12) by

$$F_M(q^2) = \int d^3x \; e^{i\vec{q}\cdot\vec{x}} \langle \mu_z(\vec{x}) \rangle , \qquad (4.21)$$

where $\langle\vec{\mu}\rangle$ is the expectation value taken with the ^{3}He ground state. Theoretical uncertainties in the treatment of the three-nucleon wave function are considerable greater than in the deuteron case. Nevertheless, there is general agreement that one-body currents alone evaluated with different types of three-body wave functions (Faddeev, Variational or "realistic" phenomenological wave functions) badly fail [38] when

confronted with data [39]. With inclusion [40] of pion exchange currents of the form discussed previously except for modifications due to nucleon form factors, the result is shown in Fig. 14, in remarkable agreement with data.

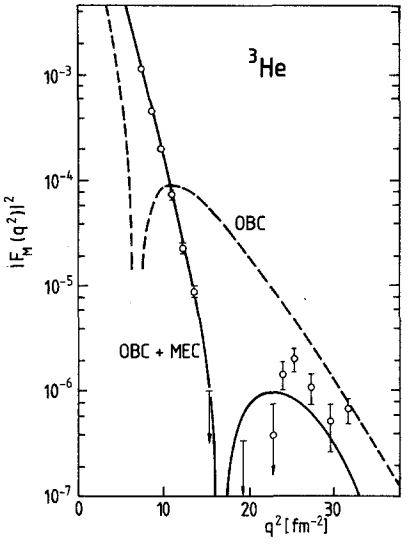

Figure 14: Magnetic form factor of ^{3}He. The dashed curve is calculated with one-body currents only. The solid line includes the effect of meson exchange currents [40]; data from [39].

LECTURE 4

5. Pion-Nucleon Scattering

In order to gain more insight into the role of the $\Delta(1232)$, and also for later purposes in treating pion-nucleus scattering, it is necessary to discuss pion-nucleon scattering, in some detail.

5.1 πN Scattering Amplitude

We write the πN elastic scattering amplitude as $f(\vec{q}',\vec{q})$, where $\vec{q}$ and $\vec{q}'$ denote in- and outgoing center-of-mass (c.m.) momenta. The differential cross section is given by $\frac{d\sigma}{d\Omega} = 1/2\,\Sigma|f|^2$, where the summation is over nucleon spins. The partial wave decomposition of $f(\vec{q}',\vec{q})$ is

$$f(\vec{q}',\vec{q}) = \sum_I Q_I \Big\{ \sum_\ell \big[(\ell+1) f_{I\ell_+}(E) + \ell f_{I\ell_-}(E)\big] P_\ell(\cos\theta) - i\vec{\sigma}\cdot(\hat{q}'\times\hat{q}) \sum_\ell \big[f_{I\ell_+}(E) - f_{I\ell_-}(E)\big] P_\ell'(\cos\theta), \tag{5.1}$$

where E is the c.m. energy, $\cos\theta = \hat{q}\cdot\hat{q}'$, Q_I projects onto the possible isospins $I = \frac{1}{2}, \frac{3}{2}$ and $\ell_\pm$ refers to channels with total angular momentum $j = \ell \pm 1/2$, respectively. The partial wave f_α ($\alpha = I\ell j$) are related to the phase shifts δ_α by

$$2iq\, f_\alpha(E) = \big[S_\alpha(E) - 1\big], \quad S_\alpha = e^{2i\delta_\alpha}. \tag{5.2}$$

A useful quantity to work with is the K matrix,

$$K_\alpha = \frac{1}{q}\tan\delta_\alpha, \quad S_\alpha = \frac{1+iqK_\alpha}{1-iqK_\alpha}, \quad f_\alpha = \frac{K_\alpha}{1-iqK_\alpha}. \tag{5.3}$$

The threshold behaviour is described by scattering lengths (a_{2I}) for s-waves and scattering volumes ($a_{2I,2j}$) for p-waves, defined by

$$a_\alpha = \lim_{q\to 0} K_\alpha / q^{2\ell}. \tag{5.4}$$

We summarize their experimental values in table 2 :

s-wave scattering lengths $[m_\pi^{-1}]$		p-wave scattering volumes $[m_\pi^{-3}]$	
a_1	0.173 ± 0.003	a_{11}	-0.081 ± 0.002
a_3	-0.101 ± 0.004	a_{13}	-0.030 ± 0.002
		a_{31}	-0.045 ± 0.002
		a_{33}	-0.214 ± 0.002

table 2: Empirical πN s-wave scattering lengths and p-wave scattering volumes, taken from ref. [41].

Note that there is a strong cancellation in the s-wave isospin-even combination $a_1 + 2a_3$ We mention that this combination vanishes in soft pion theories. Note also that the only strong channel in the p-wave is the one with spin and isospin 3/2, where a_{33} indicates strong attraction which, as we already know, supports the formation of the Δ(1232) resonance.

5.2 The Isobar Model of p-wave πN Scattering

To illustrate how the Δ(1232) enters in the p-wave πN amplitude, let us derive f_{33} in a model with nucleon, Δ(1232) and pion-baryon couplings given by eqs. (3.27 - 28). Furthermore, the simplifying assumption of static nucleons will be made. The K matrix, still keeping its operator structure in terms of nucleon spins and isospins, is then derived as follows [5,30]:

$$\langle \vec{q}'j|K|\vec{q}i\rangle = \frac{f^2}{4\pi m_\pi^2}\left[\frac{\vec{\sigma}\cdot\vec{q}'\,\vec{\sigma}\cdot\vec{q}}{-\omega}\tau_j\tau_i + \frac{\vec{\sigma}\cdot\vec{q}\,\vec{\sigma}\cdot\vec{q}'}{\omega}\tau_i\tau_j\right]$$
$$+ \frac{f_\Delta^2}{4\pi m_\pi^2}\left[\frac{\vec{S}\cdot\vec{q}'\,\vec{S}^+\cdot\vec{q}}{\omega_\Delta-\omega}T_jT_i^+ + \frac{\vec{S}\cdot\vec{q}\,\vec{S}^+\cdot\vec{q}'}{\omega_\Delta+\omega}T_iT_j^+\right], \quad (5.5)$$

where ω is the pion c.m. energy ($E = M + \omega$ in the static limit). Eq. (5.5) summarizes all direct and crossed terms with nucleon and $\Delta(1232)$ intermediate states. Note that in the K matrix, the poles appear on the real axis at the physical masses of the intermediate particles in the absence of inelasticities. The crossing symmetry is evident in eq.(5.5) by examining the invariance under the replacements $\omega \leftrightarrow -\omega$, $\vec{q} \leftrightarrow -\vec{q}'$ and $i \leftrightarrow j$, where i and j refer to the pion (cartesian) isospin indices. The energy denominator related to the $\Delta(1232)$ contains the $N\Delta$ mass difference $\omega_\Delta = M_\Delta - M = 2.1\ m_\pi$.

Projecting into the P_{33} channel and neglecting the small crossed Δ-isobar term proportional to $[\omega_\Delta + \omega]^{-1}$, we obtain

$$K_{33}(\omega) = \frac{1}{q}\tan\delta_{33} = \frac{1}{3}\frac{q^2}{4\pi m_\pi^2}\left[\frac{4f^2}{\omega} + \frac{f_\Delta^2}{\omega_\Delta-\omega}\right]. \quad (5.6)$$

If the Chew-Low value $f_\Delta = 2f$ is used, we find

$$f_{33}(\omega) = \frac{1}{q}e^{i\delta_{33}}\sin\delta_{33} = \frac{\frac{1}{3}(f_\Delta^2/4\pi m_\pi^2)\,q^2(\omega_\Delta/\omega)}{\omega_\Delta - \omega - i\,\Gamma_\Delta(\omega)/2},$$
$$\Gamma_\Delta = \frac{2}{3}\frac{f_\Delta^2}{4\pi}\frac{q^3}{m_\pi^2}\left(\frac{\omega_\Delta}{\omega}\right). \quad (5.7)$$

Here Γ_Δ is the $\Delta \to \pi N$ decay width. At resonance ($\omega = \omega_\Delta$) where $q = 1.64\ m_\pi$, one obtains $\Gamma_\Delta \simeq 130$ MeV which is not far from the experimental width ($\Gamma_\Delta = 115 \pm 5$ MeV).

For a quantitative description of the p-wave πN phase shifts, the static limit is not accurate enough. Relativistic kinematics has to be treated appropriately, and inclusion of the N*(1470) in the spin-isospin 1/2 channel is necessary to reproduce the correct energy dependence of the P_{11} phase shift. Details are given in ref. [5]. Relativistic corrections can effectively be absorbed in the πNN and $\pi N\Delta$ coupling Hamiltonians, eqs. (3.27 - 28) by multiplying a factor $(2M/M + E)^{1/2}$ and $(2M_\Delta/M_\Delta + E)^{1/2}$, respectively The experimental $\Delta \to \pi$N width is then obtained with $f_\Delta^2/4\pi = 0.37$.

The p-wave phase shifts obtained in such a refined isobar model are shown in Fig. 15. We conclude that a p-wave π-nucleon K matrix with masses of the free nucleon, Δ and N*, is an appropriate starting point for subsequent discussions of pion-nucleus interactions.

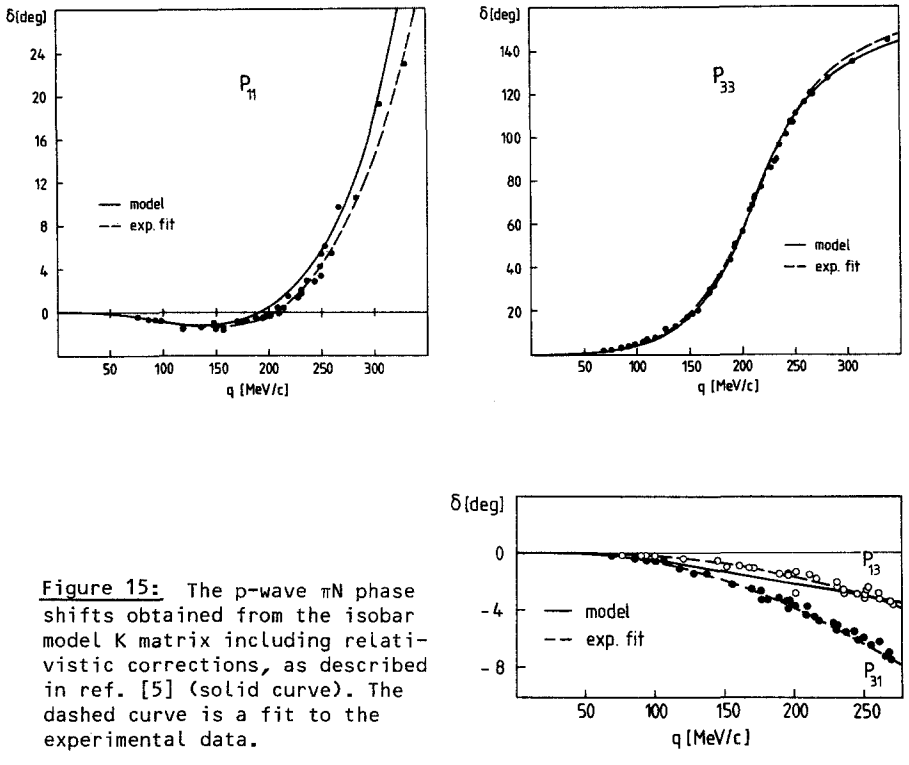

Figure 15: The p-wave πN phase shifts obtained from the isobar model K matrix including relativistic corrections, as described in ref. [5] (solid curve). The dashed curve is a fit to the experimental data.

LECTURE 5

6. Pions in Nuclear Matter

6.1 Introduction: the Pion Propagator

This section is intended to prepare some of the basic concepts for the treatment of the pion-nucleus many-body problem, following ref. [5]. The framework to start with is defined by a Hamiltonian

$$H = H_N + H_\Delta + H_\pi + H_{\pi NN} + H_{\pi N\Delta} , \tag{6.1}$$

where H_N, H_Δ and H_π correspond to free nucleons, $\Delta(1232)$ and pions, $H_{\pi NN}$ and $H_{\pi N\Delta}$ are the π-nucleon and $\pi N\Delta$-coupling Hamiltonians, eq. (3.27-28).

The pion field in the medium obeys the equation

$$(\Box + m_\pi^2)\ \vec{\phi}(\vec{r},t) = \vec{J}_5(\vec{r},t), \tag{6.2}$$

where $\vec{J}_5$ is the isovector, pseudoscalar pion source function. In the absence of sources, the free pion field is written in second quantized form as

$$\phi^{\lambda}(\vec{r},t) = \int \frac{d^3q}{(2\pi)^{3/2}} \frac{1}{\sqrt{2\omega}} \left[a_{q\lambda} e^{-i(\omega t - \vec{q}\cdot\vec{r})} + a^{+}_{q\lambda} e^{i(\omega t - \vec{q}\cdot\vec{r})} \right], \quad (6.3)$$

where $\omega = \omega(\vec{q}) = \sqrt{\vec{q}^2 + m_\pi^2}$ and λ denotes isospin. For a pion in a nuclear medium, the spectrum $\omega(\vec{q})$ will change due to the interactions with the medium.

The pion propagator D is defined by

$$i\,\delta_{\lambda\lambda'}\, D(\vec{r},\vec{r}';t) = \langle 0 | T\, \phi^{\lambda}(\vec{r},t)\, \phi^{\lambda}(\vec{r}',0) | 0 \rangle, \quad (6.4)$$

where T denotes the time-ordered product, and the vacuum refers to the many-body ground state. It is convenient to work in momentum space and express D in terms of the free pion propagator.

$$D_0(\omega,\vec{q}) = \int \frac{d^4x}{(2\pi)^4} e^{iq\cdot x} D_0(\vec{x},0;t) = \left[\omega^2 - \vec{q}^2 - m_\pi^2 + i\delta\right]^{-1}, \quad (6.5)$$

by

$$D(\omega,\vec{q}) = D_0(\omega,\vec{q}) + D_0(\omega,\vec{q})\,\Pi(\omega,\vec{q})\,D(\omega,\vec{q}) \quad (6.6)$$

$$= \left[\omega^2 - \vec{q}^2 - m_\pi^2 - \Pi(\omega,\vec{q}) + i\delta\right]^{-1}.$$

This defines the pion self-energy $\Pi(\omega,\vec{q})$ which can be interpreted as the "potential" experienced by the pion due to the interactions with the medium.

The singularities of $D(\omega,\vec{q})$ determine the spectrum $\omega(\vec{q})$ of excitations carrying the quantum numbers of the pion. The pionic response function, or pseudoscalar-isovector current correlation function, is defined by

$$\delta_{\lambda\lambda'}\, R(\vec{r},\vec{r}';t) = \langle 0 | T\, J_5^{\lambda}(\vec{r},t)\, J_5^{\lambda'}(\vec{r}',0) | 0 \rangle. \quad (6.7)$$

In momentum space, the response function is obtained from the pion self-energy by

$$R(\omega,\vec{q}) = \Pi(\omega,\vec{q}) + \Pi(\omega,\vec{q})\,D_0(\omega,\vec{q})\,R(\omega,\vec{q})$$

$$= \Pi(\omega,\vec{q}) + \Pi(\omega,\vec{q})\,D(\omega,\vec{q})\,\Pi(\omega,\vec{q}). \quad (6.8)$$

The quantity of primary interest is clearly the pion self-energy $\Pi(\omega,\vec{q})$ which summarizes all (irreducible) interactions of the pion with the medium.

6.2. Pion-Selfenergy and related quantities

We consider now the pionic response of an infinite medium with equal number of protons and neutrons. The pion field has energy ω and momentum $\vec{q}$. Following the discussion of previous chapters, we expect that the pion field will polarize the medium primarily via the p-wave πN interaction by exciting either nucleon-hole or $\Delta(1232)$-hole states.

A first order picture of the response is then given by the pion self-energy $\Pi^{(o)}$ illustrated in Fig. 16. We write it, somewhat schematically, as

$$\Pi^{(o)}(\omega,\vec{q}) = -\sum_{Nh} \frac{|\langle\pi(q)|H_{\pi NN}|Nh\rangle|^2}{\varepsilon_N - \varepsilon_h - \omega} + \text{crossed term} - \sum_{\Delta h} \frac{|\langle\pi(q)|H_{\pi N\Delta}|\Delta h\rangle|^2}{\varepsilon_\Delta - \varepsilon_h - \omega} + \text{crossed term} \quad . \tag{6.9}$$

Here $|Nh\rangle$ and $|\Delta h\rangle$ denote a nucleon-hole or Δ-hole state carrying pion quantum numbers, and ε_Δ, ε_N, ε_h are the corresponding single particle energies.

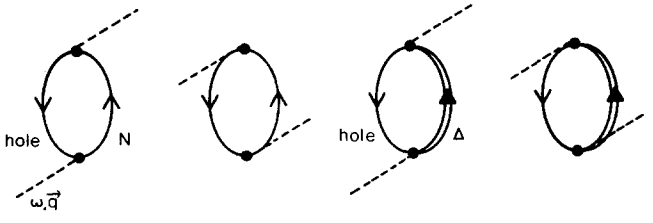

Figure 16: Lowest order p-wave pion selfenergy through nucleon-hole and $\Delta(1232)$-hole excitations.

We rewrite eq. (6.9) as

$$\Pi^{(o)}(\omega,\vec{q}) = -\vec{q}^{\,2}\,\mathring{\chi}(\omega,\vec{q}) \,, \tag{6.10}$$

where the factor $\vec{q}^{\,2}$ is due to the p-wave nature of the interaction. This defines the lowest order pionic susceptibility $\mathring{\chi}$ of the medium. Because of the spin-dependence of the underlying interaction it is useful to point out [42] the analogy between the pionic response problem and the one encountered in magnetic materials. In that sense, $\mathring{\chi}$ has a "diamagnetic" part $\mathring{\chi}_\Delta$ which involves high-lying Δ-hole excitations and a "paramagnetic" component $\mathring{\chi}_N$ related to low lying nucleon-hole excitations.

The explicit form of $\mathring{\chi} = \mathring{\chi}_N + \mathring{\chi}_\Delta$ for symmetric nuclear matter is as follows:

$$\mathring{\chi}_N(\omega,\vec{q}) = \frac{4f^2(q^2)}{m_\pi^2}\int\frac{d^3p}{(2\pi)^3}\,\frac{n(\vec{p})[1-n(\vec{p}+\vec{q})]}{\varepsilon(\vec{p}+\vec{q})-\varepsilon(\vec{p})-\omega-i\delta} + \text{crossed term} \tag{6.11}$$

where the factor of 4 comes from the spin-isospin sum, $n(\vec{p})$ is unity for $|\vec{p}| \leq k_F$, the Fermi momentum, and zero otherwise, and $\varepsilon(\vec{p}) = \vec{p}^{\,2}/2M^*$, where M^* is the nucleon effective mass. The crossed term is obtained from the direct one by the replacements $\omega \to -\omega$ and $\vec{q} \to -\vec{q}$. The integral eq. (6.11) can be worked out analytically. The result is given in ref. [43]. For large pion frequencies ω and low nuclear densities ρ, one finds

$$\mathring{\chi}_N(\omega,q) \simeq \frac{f^2(q^2)}{m_\pi^2}\left[\frac{\rho}{q^2/2M^*-\omega} + \frac{\rho}{q^2/2M^*+\omega}\right]. \qquad (6.12)$$

Note that $\mathring{\chi}_N(\omega,q) \to 0$ as $M^* \to \infty$, so that in this limit the pionic response for symmetric nuclear matter is completely determined by $\Delta(1232)$ excitations. This applies, in particular, for $\omega \gtrsim m_\pi$, the kinematic region of pionic atoms and low energy pion-nucleus scattering. At $\omega = 0$ and $q < k_F$, one finds

$$\mathring{\chi}_N(\omega=0,q) = \frac{f^2(q^2)}{m_\pi^2}\frac{2M^*k_F}{\pi^2}\left[1 - \frac{1}{12}\frac{q^2}{k_F^2} + \ldots\right]. \qquad (6.13)$$

To leading order, $\mathring{\chi}_N(\omega = 0, \vec{q} \to 0)$ is then determined by the density of states at the Fermi surface, $2M^*k_F/\pi^2$.

The $\Delta(1232)$-hole susceptibility $\mathring{\chi}_\Delta$ is

$$\mathring{\chi}_\Delta(\omega,q) = \frac{16}{9}\frac{f_\Delta^2(q^2)}{m_\pi^2}\int\frac{d^3p}{(2\pi)^3}\frac{n(\vec{p})}{\varepsilon_\Delta(\vec{p}+\vec{q})-\varepsilon(\vec{p})-\omega} + \text{crossed terms}. \qquad (6.14)$$

In the absence of Δ-interactions other than those responsible for free $\Delta \to \pi N$ decay,

$$\varepsilon_\Delta(\omega,\vec{p}) = M_\Delta - M + \frac{\vec{p}^2}{2M_\Delta} - \frac{i}{2}\Gamma_\Delta(\omega). \qquad (6.15)$$

At large pion energies ($\omega >> q^2/2M$), one obtains

$$\mathring{\chi}_\Delta(\omega,q) \simeq \frac{4}{9}\frac{f_\Delta^2(q^2)}{m_\pi^2}\left[\frac{\rho}{\omega_\Delta-\omega-i\Gamma_\Delta(\omega)/2} + \frac{\rho}{\omega_\Delta+\omega}\right], \qquad (6.16)$$

where $\omega_\Delta = M_\Delta - M \simeq 2.1\ m_\pi$. At $\omega = 0$, $\mathring{\chi}_N$ dominates the pionic susceptibility, but

$$\mathring{\chi}_\Delta(\omega=0,q) = \frac{8}{9}\frac{f_\Delta^2(q^2)}{m_\pi^2}\frac{\rho}{\omega_\Delta} \qquad (6.17)$$

still gives a contribution of about 35 % to the total $\mathring{\chi}$.

6.3 The Optical Potential and the Diamesic Function

For $\omega \gtrsim m_\pi$, the "pion optics" domain explored by pion elastic scattering, it is convenient to work with an optical potential. The lowest order p-wave optical potential is related to the pion self-energy simply by

$$U_{opt}^{(o)}(\omega,q) = \frac{1}{2\omega}\Pi^{(o)}(\omega,q) = -\frac{4\pi}{2\omega}q^2c_o\rho. \qquad (6.18)$$

The quantity c_o is the spin-isospin averaged scattering volume; at threshold ($\omega = m_\pi$),

$$c_o = \frac{1}{3}\left[4a_{33} + 2a_{13} + 2a_{31} + a_{11}\right] = 0.21\ m_\pi^{-3} \qquad (6.19)$$

in terms of the p-wave scattering volumes, table 2. Recalling from eqs. (6.12, 6.16) that only $\mathring{\chi}_\Delta$ contributes at $\omega = m_\pi$, $q \to 0$, one finds

$$c_0(\omega=m_\pi, q=0) = \frac{8}{9}\frac{f_\Delta^2}{4\pi m_\pi^2}\frac{\omega_\Delta}{\omega_\Delta^2 - m_\pi^2}, \tag{6.20}$$

which is quite close to eq. (6.19).

The response function in this simplest possible model is obtained by iteration of $\Pi^{(o)}$ with pure one-pion exchange:

$$R(\omega,q) = \Pi^{(o)}(\omega,q) + \Pi^{(o)}(\omega,q)\frac{1}{\omega^2 - q^2 - m_\pi^2} R(\omega,q). \tag{6.21}$$

It is convenient to summarize the medium effects in a diamesic function $\varepsilon(\omega,q)$ [5,44]:

$$R(\omega,q) = \frac{\Pi^{(o)}(\omega,q)}{\varepsilon(\omega,q)}. \tag{6.22}$$

From eqs. (6.21), (6.10) one obtains the standard RPA result

$$\varepsilon(\omega,q) = 1 + \frac{q^2}{\omega^2 - q^2 - m_\pi^2}\chi^\circ(\omega,q). \tag{6.23}$$

The zeros of ε determine the spectrum $\omega(q)$ of pion-like excitations.

In the optical part of the spectrum, a complex index of refraction n for pions can be defined by

$$n^2 = \frac{q^2}{\omega^2 - m_\pi^2} = \frac{1}{1 - \chi(\omega,q)}. \tag{6.24}$$

The pion scattering T-matrix is simply given by $T = R/2\omega$. This T matrix, with eq. (6.21, 22) represents the multiple scattering expansion with the first order p-wave optical potential.

The properties of the diamesic function $\varepsilon(\omega,q)$ have been discussed in great detail in the literature. One particularly interesting question is whether the nuclear medium can act as an amplifier for the pion field at no cost of energy. To find this out, let us discuss the diamesic function at zero frequency. By examining eq. (6.23) one sees that $\varepsilon(\omega = 0, q)$ can approach values small compared to unity at sufficiently large q and sufficiently high density. In fact, as $\varepsilon \to 0$ for $\omega = 0$ a pionic soft mode develops which indicates a phase transition into a pion condensate [45, 46].

For the simple model described above the particle-hole interaction which drives pionic modes is entirely given by one-pion exchange. The OPE tensor force is sufficiently attractive at high momentum transfers ($q_c \sim 2\text{-}3\ m_\pi$) so that in the absence of repulsive correlations, the condition $\varepsilon \to 0$ is actually met at critical densities ρ_c which are only a fraction of nuclear matter density, $\rho_o = 0.17\ \text{fm}^{-3}$. Obviously, the picture is much oversimplified up to this point, since there seem to be no traces of critical pionic phenomena in nuclei.

LECTURE 6

6.4 Spin-Isospin dependent Particle-Hole Interaction

We proceed now to discuss spin-isospin correlations other than one-pion exchange. For later purposes, we shall not only consider here pionic modes of excitation, those driven by spin-longitudinal interactions of the type $\vec{\sigma}_1 \cdot \vec{q}\ \vec{\sigma}_2 \cdot \vec{q}$, but also spin-transverse ones. The particle-hole interaction in spin-isospin excitation channels must be of the general form (in momentum space, and in direct particle-hole channels):

$$V_{\sigma\tau}(\omega,\vec{q}) = \left[W_\ell(\omega,q)\,\vec{\sigma}_1\cdot\hat{q}\,\vec{\sigma}_2\cdot\hat{q} + W_t(\omega,q)(\vec{\sigma}_1\times\hat{q})\cdot(\vec{\sigma}_2\times\hat{q})\right]\vec{\tau}_1\cdot\vec{\tau}_2 . \qquad (6.25)$$

We ignore spin-orbit interactions which are empirically small in isovector channels. Note that an equivalent formulation of eq. (6.25) is:

$$V_{\sigma\tau} = \left\{\left[\tfrac{1}{3}W_\ell + \tfrac{2}{3}W_t\right]\vec{\sigma}_1\cdot\vec{\sigma}_2 + \left[\tfrac{1}{3}W_\ell - \tfrac{1}{3}W_t\right]S_{12}(\hat{q})\right\}\vec{\tau}_1\cdot\vec{\tau}_2 . \qquad (6.26)$$

Eqs. (6.25, 26) have been written down for nucleons; for Δ's the appropriate replacements $\vec{\sigma}\to\vec{S}^+$ and $\vec{\tau}\to\vec{T}^+$ have to be made.

The prototype of the longitudinal interaction W_ℓ is one-pion exchange. As in the previous section, for large energy transfers ω, one has to go beyond the static approximation and include retardation:

$$W_\pi(\omega,q) = \frac{f^2(q^2)}{m_\pi^2}\,\frac{q^2}{\omega^2 - q^2 - m_\pi^2 + i\delta} , \qquad (6.27)$$

with f replaced by f_Δ if N-Δ transitions are involved. This is how far one can go in a model based on the Hamiltonian, eq. (6.1). In the hierarchy of interactions, W_π of eq. (6.27) represents the well established long-range part; the less well established shorter range contributions will now have to be discussed in some detail. In fact, much of the presently ongoing debate is about uncertainties at the level of short-range spin-isospin correlations.

The prototype of the transverse coupling interaction W_t is isovector two-pion exchange, usually in its simplified ρ-exchange version, following eq. (2.8):

$$W_\rho(\omega,q) = \frac{f_\rho^2}{m_\rho^2}\,\frac{q^2}{\omega^2 - q^2 - m_\rho^2} . \qquad (6.28)$$

We have mentioned previously that the short range behaviour of eq. (6.28) is too simplistic because of strong cutoff corrections at high momentum transfers [47] which act differently in spin-spin and tensor channels. In actual calculations, such cutoffs have been introduced phenomenologically [48,49]. In any case, one expects the prototype interactions to be accompanied by screening effects at short distances from several possible sources:

(a) repulsive short-range correlations, or alternatively: effects from quark-gluon

dynamics at short distances;

(b) many-body vertex corrections, e.g. from exchange terms.

Within the framework of Landau-Migdal theory [50,51], these screening effects are altogether summarized in terms of a phenomenological repulsive Fermi-liquid interaction,

$$g' \vec{\sigma}_1 \cdot \vec{\sigma}_2 \; \vec{\tau}_1 \cdot \vec{\tau}_2 \; , \tag{6.29}$$

to be added to the prototype interactions. Actually, $g' = g'(\omega,q)$ is a function of ω and q as well; if the underlying interactions are short ranged, one expects this dependence to be smooth.

Additional tensor correlation pieces of the type $h'(\omega,q)\; S_{12}(\hat{q})\vec{\tau}_1 \cdot \vec{\tau}_2$ have also been discussed in the literature and found to be small compared to the leading pieces from π and ρ exchange [53] but the question might have to be reopened in the light of more complete many-body calculations [54].

The magnitude of g' will turn out to be of crucial importance in all subsequent discussions. Note that g' acts in the same way in longitudinal and transverse channels, since $\vec{\sigma}_1 \cdot \vec{\sigma}_2 = \vec{\sigma}_1 \cdot \hat{q}\; \vec{\sigma}_2 \cdot \hat{q} + (\vec{\sigma}_1 \times \hat{q}) \cdot (\vec{\sigma}_2 \times \hat{q})$. Hence for the static interaction $V_{\sigma\tau}(\omega=0)$, the following ansatz results:

$$W_\ell(q^2) = g' - \frac{f^2}{m_\pi^2} \frac{q^2}{q^2+m_\pi^2} \; ; \; W_t(q^2) = g' - \frac{f_\rho^2}{m_\rho^2} \frac{q^2}{q^2+m_\rho^2} \; . \tag{6.30}$$

The static long-wavelength spin-isospin response is entirely determined by g', since

$$V_{\sigma\tau}(\omega=0, q=0) = g' \vec{\sigma}_1 \cdot \vec{\sigma}_2 \; \vec{\tau}_1 \cdot \vec{\tau}_2 \; , \tag{6.31}$$

and g' is related, up to a constant, to the Landau-Migdal Fermi liquid parameter G_0'. If this identification is made, g' already includes exchange terms of the particle-hole interaction by definition, so that only direct particle-hole matrix elements should be calculated with $V_{\sigma\tau}$.

Information about g' for nucleons is obtained from investigations of various magnetic nuclear properties within the Landau-Migdal framework. Commonly accepted values are [+] $g' = 0.6 - 0.7$ [52,53]. Reaction matrix calculations starting from realistic nucleon-nucleon interactions come close to such numbers, and they also show that g' is a smooth function of momentum transfer q [54]. At a more phenomenological level [5], similar values of g' can be obtained in a model where $V_{\sigma\tau}$ is made of π and ρ exchange times a two-body correlation function which approximates Brueckner reaction matrix calculations.

6.5 The Lorentz-Lorenz Correction, and g' from a Chiral Bag Model point of view

The Lorentz-Lorenz (LL) correction [55] has always been subject to a great deal of interest as a prototype many-body effect in pion-nucleus interactions. The classical

+) We give values of g' in pionic units, i.e. in units of $(f/m_\pi)^2$.

LL effect is equivalent to $g' = 1/3$; it simply corresponds to the removal of the δ-function piece from V_π of eq. (27) in the presence of a repulsive core [56]. This effect can be given a simple interpretation [57] from the point of view of chiral bag models. In the simplest version of such models, the space inside the bag is occupied by quarks, but no pions, while the pion field exists outside the bag and joins to the quark axial current at the boundary such as to make it continuous across the boundary. The axial current is

$$\vec{A}^\lambda = \bar{q}\,\vec{\gamma}\,\gamma_5\,\frac{\tau^\lambda}{2}\,q\;\theta(R-r) + f_\pi\,\vec{\nabla}\,\phi^\lambda\;\theta(r-R), \tag{6.32}$$

where the q are quark fields and R is the bag radius. For zero pion mass, the axial current is conserved, $\vec{\nabla}\cdot\vec{A} = 0$, which imples that on the bag boundary,

$$\bar{q}\,\vec{\gamma}\,\gamma_5\,\frac{\tau^\lambda}{2}\,q\cdot d\vec{S} = f_\pi\,\vec{\nabla}\,\phi^\lambda\cdot d\vec{S} \tag{6.33}$$

for each surface element normal to the bag sphere.

Let us consider now a medium of well separated bags. We wish to rederive the classical Lorentz-Lorenz correction assuming that the average distance between the bags is large at the boundary of a given bag differs from the field in free space by the spin-isospin polarizability of the medium. Therefore, in the space between bags, the pion field equation $\nabla^2\phi = 0$ is modified in first order according to $\vec{\nabla}(1-\chi)\vec{\nabla}\phi = 0$, where χ is the pionic susceptibility, eq. (6.10). Consequently the boundary condition, eq. (6.33), becomes

$$\frac{1}{f_\pi}\,\bar{q}\,\vec{\gamma}\,\gamma_5\,\frac{\tau^\lambda}{2}\,q\cdot d\vec{S} = (1-\chi)\,\vec{\nabla}\,\phi^\lambda\cdot d\vec{S}\,. \tag{6.34}$$

The local field correction, $\delta\vec{\nabla}\phi\cdot d\vec{S} = -\chi\,\vec{\nabla}\phi\cdot d\vec{S}$, has to be averaged over angles which gives a factor 1/3. Performing the correction to all orders yields the local field at the bag boundary

$$\phi_{loc} = \frac{\phi_0}{1+\frac{1}{3}\chi} \tag{6.35}$$

where ϕ_0 is the pion field in free space. The factor $(1+\chi/3)^{-1}$ is equivalent to a Landau-Migdal parameter $g' = 1/3$, the classical Lorentz-Lorenz correction, obtained here simply because of the total screening of medium polarization effects from the baryon interior due to the confining forces keeping the quarks inside. Eq. (6.35) still holds if $q\bar{q}$ components carrying pion quantum numbers are allowed inside the bag, such as in the Cloudy Bag model (A.W. Thomas [16]), as long as the confining boundary provides a perfect screening of the baryon interior against the spin-isospin polarization effects in the many-body medium surrounding this baryon.

The significance of this simple model is that it obviously provides a universal g' for both nucleons and Δ-isobars (after separating trivial spin-isospin factors), thereby maintaining the underlying SU(4) symmetry of the problem. We regard this g' as the "minimal" one, expected to be present in any nuclear medium with non-overlapping bags.

Additional contributions to g' are expected to come from short-range dynamics involving overlapping bags.

In discussions of the Landau-Migdal parameter g'_Δ for Δ's, two different positions are presently taken:

(a) the universality hypothesis, based in one or another form on the above quark model considerations and their underlying spin-isospin SU(4) symmetry. In this picture, $g'_\Delta = g'_N$ is assumed;

(b) arguments based on one-boson exchange NΔ-interactions with phenomenological cutoffs, but otherwise treating nucleon and $\Delta(1232)$ as elementary particles. In such models, exchange terms of the short-range NΔ-interactions tend to cancel direct terms [58], such that the resulting g'_Δ is substantially smaller than g'_N.

Both approaches are probably too simple to be realistic. The universality argument may well hold for the classical LL correction, $g' = 1/3$, which represents one half of the empirical g' for nucleons. The question is whether the other half, e.g. from overlapping bags, follows the same universality rule. On the other hand, the treatment of the short-distance exchange terms of the NΔ force as if N and Δ were elementary particles is similarly questionable. In a situation like this, we shall strictly follow the Landau-Migdal framework and treat g'_Δ as phenomenological parameter.

6.6 Summary: Spectrum of Pion-like Excitations in Nuclear Matter

With incorporation of correlations other than one-pion exchange, pion self-energy is turned into

$$\Pi = \frac{-q^2 \mathring{\chi}}{1 + g' \mathring{\chi}} , \tag{6.36}$$

and the diamesic function becomes

$$\varepsilon(\omega,q) = 1 + \left[\frac{q^2}{\omega^2 - q^2 - m_\pi^2} + g' \right] \mathring{\chi} . \tag{6.37}$$

The presence of a positive (repulsive) g' raises the critical density ρ_{crit} for a pionic instability. We show this in Fig. 17. For $g' = 0.6 - 0.7$, ρ_{crit} is raised beyond three to five times nuclear matter density, which moves both pion condensates and its precursors far away from experimentally explorable domains.

To summarize this section, we present in Fig. 18 a schematic picture of the spectrum $\omega(q)$ of pionic excitations in nuclear matter determined by the condition $\varepsilon(\omega,q) = 0$, i.e. by the singularities of the pion-nuclear response function $R(\omega,q)$. The following domains are of particular interest:

(I) The area of low-energy π-nucleus scattering and pionic atoms. The issue there is to learn about many-body corrections to the first order pion-nucleus optical potential (such as the Lorentz-Lorenz correction and other effects).

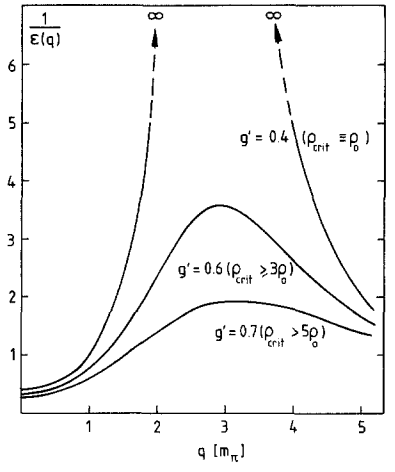

Figure 17: The inverse static diamesic function $\varepsilon^{-1}(\omega = 0, q)$. Shown is the dependence on the Landau parameter g'.

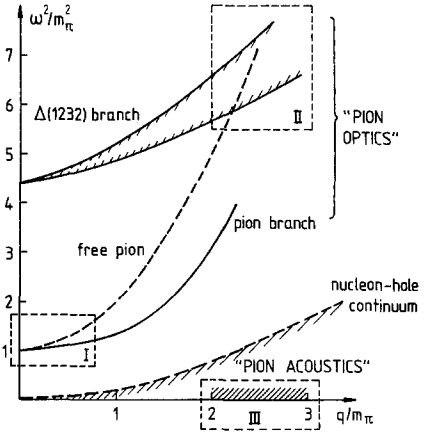

Figure 18: Schematic picture of the various pionic modes of excitation in nuclear matter, as explained in the text.

(II) The region of $\Delta(1232)$ propagation. Here the interest is in the interactions of the Δ with surrounding nucleons, resulting in a change of its mass and decay width (indicated by the broad band associated with the $\Delta(1232)$ branch in Fig. 18).

(III) The domain of possible pionic soft-modes embedded into the continuum of low frequency pion-like nucleon-hole excitations. For sufficiently large g', such soft mode behaviour is essentially ruled out, as mentioned before.

(IV) The low frequency, long wavelength limit where according to Fig. 17 one expects of spin-isospin dependent response. The amount of quenching is determined by $g'(\omega = 0, q = 0)$.

LECTURE 7

7. Nuclear Spin-Isospin Response

7.1 Introduction

We wish now to follow the conceptual framework developed for nuclear matter and adapt it to finite nuclei. At the same time we generalize the scheme to describe spin-isospin response problems not only of pionic type, but also with spin-transverse operators.

Following previous discussions, we recall that there exist two basic types of spin-isospin excitation mechanisms in nuclei:

(1) Nucleonic transitions involving the excitation of the Δ(1232) by spin-isospin flip at the quark level (see Fig. 19a). In many-body language, these are Δ-hole excitations. (2) Nuclear spin-isospin transitions involving spin-flip, ΔT = 1 nucleon-hole excitations (see Fig. 19b).

At first sight, these two types of excitations would appear to be rather unrelated, because of the very different energy scales involved: the scale for Δ hole excitations is determined by the Δ-N mass difference of about 300 MeV, whereas the characteristic energy of the relevant nucleon-hole states is given by the energy spacing between $j_>$ and $j_<$ spin-orbit partners or their analogues, typically of order 10 MeV.

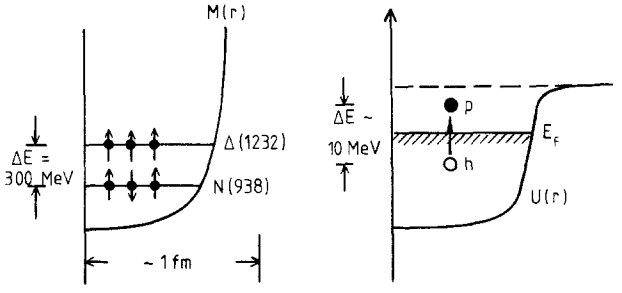

Figure 19: Illustration of spin-isospin excitation mechanisms
(a) N→Δ transition at the quark level;
(b) Isovector-spinflip nucleon-hole excitation

On the other hand, one must keep in mind that N-Δ transitions are strong, following developments in previous chapters, and that the suppression by a large energy denominator can be partly compensated by a large coupling strength. One expects therefore that there will be a coupling between nucleon-hole and Δ-hole modes, even at low energy. The degree to which this coupling occurs will depend on the strength of N-Δ interactions.

The main problem in discussing the role of the Δ(1232) in low energy nuclear spin-isospin transitions is to discriminate its effects from standard core polarization induced by strong tensor correlations [59]. These core polarization mechanisms involve virtual nuclear excitations at similar energy scale (i.e. several hundred MeV) as Δ-hole excitations, hence one expects that both effects have to be discussed at the same level.

7.2 Spin-Isospin Response Function

We shall consider two basic types of spin-isospin operators :

$$F_\ell = \sum_{j=1}^{A} \vec{\sigma}_j \cdot \hat{q}\ \tau_j^\lambda\ e^{i\vec{q}\cdot\vec{r}_j}, \qquad \text{(longitudinal)} \quad (7.1)$$

$$F_t = \sum_{j=1}^{A} (\vec{\sigma}_j \times \hat{q})_z\ \tau_j^\lambda\ e^{i\vec{q}\cdot\vec{r}_j}. \qquad \text{(transverse)} \quad (7.2)$$

The terms "longitudinal" and "transverse" indicate the preferred alignment between spin and momentum transfer q. For N-Δ-transitions the replacements $\vec{\sigma} \to \vec{S}^{+}$ and $\vec{\tau} \to \vec{T}^{+}$ are to be made. Excitations driven by F_ℓ are called "pion-like" because of their pseudoscalar-isovector nature. Transverse excitations via F_t are encountered in magnetic isovector-spin transitions. The (p,n) and (p,p′) reactions involve combinations of both F_ℓ and F_t.

It is convenient to introduce the response function (or susceptibility) of the nuclear many-body system with respect to a perturbing spin-isospin operator F, in close analogy with developments in section 6.1:

$$R_F(\vec{q}',\vec{q};\omega) = \sum_n \left\{ \frac{\langle 0|F^+(\vec{q}')|n\rangle\langle n|F(\vec{q})|0\rangle}{\omega - E_n + i\delta} - \frac{\langle 0|F^+(-\vec{q})|n\rangle\langle n|F(-\vec{q}')|0\rangle}{\omega + E_n} \right\}, \tag{7.3}$$

where $|0\rangle$ and $|n\rangle$ are the nuclear ground state and excited states, respectively, and E_n are the excitation energies. For a finite nucleus, the in- and outgoing momenta $\vec{q}$ and $\vec{q}'$ can be different, unlike the situation in nuclear matter.

The strength function is defined by

$$S_F(\vec{q},\omega) = -\frac{1}{\pi}\, Im\, R_F(\vec{q},\vec{q};\omega) = \sum_n \delta(\omega - E_n)\,|\langle n|F(\vec{q})|0\rangle|^2. \tag{7.4}$$

In scattering experiments like (e,e′), (p,p′) or (p,n), the differential cross section is proportional to S_F:

$$\frac{d^2\sigma}{d\Omega\, dE} \propto S_F(\vec{q},\omega). \tag{7.5}$$

In pion or photon scattering, the scattering amplitude is directly proportional to R_F. For example, the pion-nucleus amplitude f is obtained by identifying $F \equiv \delta H = H_{\pi NN} + H_{\pi N\Delta}$:

$$f(\theta,\omega) = -\frac{1}{4\pi} \sum_n \frac{\langle 0|\delta H^+(\vec{q}')|n\rangle\langle n|\delta H(\vec{q})|0\rangle}{\omega - E_n + i\delta} + \text{crossed term}, \tag{7.6}$$

and the total cross section is

$$\sigma(\omega) = \frac{4\pi}{q}\, Im\, f(\theta=0,\omega). \tag{7.7}$$

7.3 First Order Response

The elementary mode of nuclear polarization is given by particle-hole (either nucleon-hole or Δ-hole) excitations $|ph\rangle$ coupled to the appropriate quantum numbers:

$|Nh\rangle = |(\text{nucleon-hole})\ J^\pi, \Delta T = 1\rangle$,

$|\Delta h\rangle = |(\Delta(1232)\text{-hole})\ J^\pi, \Delta T = 1\rangle$.

The lowest order response is described by:

$$\mathring{R}_F = \langle 0 | F^+ G_0(\omega) F | 0 \rangle, \tag{7.8}$$

where

$$G_0 = G_0^N + G_0^\Delta .$$

Here

$$G_0^N(\omega) = \sum_{Nh} |Nh\rangle \left[\frac{1}{\omega - \varepsilon_N + \varepsilon_h + i\delta} - \frac{1}{\omega + \varepsilon_N - \varepsilon_h - i\delta} \right] \langle Nh| \tag{7.9}$$

is the nucleon-hole Green's function. We now choose ε_N and ε_h, the single particle energies as eigenvalues of an appropriate Hartree-Fock Hamiltonian H_0. The Δ-hole Green's function is

$$G_0^\Delta(\omega) = \sum_{\Delta h} |\Delta h\rangle \left[\frac{1}{\omega - E_{\Delta h}(\omega)} - \frac{1}{\omega + E_{\Delta h}(-\omega)} \right] \langle \Delta h| , \tag{7.10}$$

where the Δ-hole energy is a complex function of the excitation energy ω, as in eq. (6.15), but modified by possible Hartree-Fock type binding effects.

7.4 Response Function in the RPA approximation

The next step beyond single particle response is by introduction of the spin-isospin particle-hole interaction, see section 6.4. The frequently used RPA approximation corresponds to iterating the process, Fig. 20, to all orders:

$$\begin{aligned} R_F^{RPA} &= \langle 0 | F^+ [G_0(\omega) + G_0(\omega)\, V\, G_0(\omega) + \ldots] F | 0 \rangle \\ &= \langle 0 | F^+ \frac{G_0(\omega)}{1 - V G_0(\omega)} F | 0 \rangle . \end{aligned} \tag{7.11}$$

For pion-nucleus scattering, we recall that this is equivalent to summing the multiple scattering series with the first order optical potential.

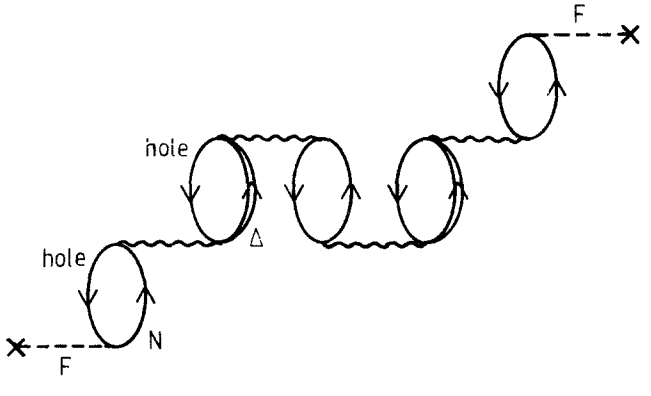

Figure 20: Graphical illustration of the response function within RPA

7.5 Two-Particle-Two-Hole Contributions

The one-particle-one-hole RPA framework described above is not sufficient to provide a realistic description of the response function at large energy transfers. The 1p1h states couple strongly to the 2p2h continuum. As we shall see, this is the leading mechanism for pion absorption in nuclei which proceeds mainly on nucleon pairs.

Such corrections provide an additional width and shift to the nucleon-hole or Δ-hole states. To illustrate this, let $|ph\rangle$ be a particle-hole state and $|\lambda\rangle = |2N2h\rangle$ a two-nucleon-two-hole continuum state. We denote by V the interaction which couples these states. Second order perturbation theory leads to a complex shift of the particle-hole energy

$$\delta E_{ph} = \sum_{\lambda} \frac{|\langle ph|V|\lambda\rangle|^2}{E_o - E_\lambda - i\delta}\,, \tag{7.12}$$

where the sum over λ is understood as an integration over E_λ, and E_o is the starting energy, given essentially by the energy transfer ω to the nucleus. If E_o is larger than the two-nucleon emission threshold, we obtain an energy dependent width

$$\langle ph|\Gamma_{2p2h}|ph\rangle = -2\,Im\,\delta E_{ph}\,. \tag{7.13}$$

This width contributes to the imaginary part of the response function.

Later on we shall discuss the influence of such absorptive mechanisms on the pion-nucleus cross section. Here we would like to give an impression of the relative size of 2p2h contributions to the response function by examining the transverse structure function $S_T(\omega,q)$ derived from inclusive inelastic electron scattering.

The differential cross section for single arm (e,e') measurement with one-photon exchange is

$$\frac{d^2\sigma}{d\Omega\,dE'} = K\sigma_{Mott}\left\{\left(\frac{q_\mu^2}{\vec{q}^2}\right)^2 S_L(\omega,q) + \left[\left(\frac{q_\mu^2}{\vec{q}^2}\right) + tan^2\frac{\theta}{2}\right]S_T(\omega,q)\right\}, \tag{7.14}$$

where K is a kinematical factor and $q_\mu^2 = \omega^2 - \vec{q}^2$. At backward angles, the transverse structure function S_T can be separated from the longitudinal one, S_L. This S_T measures the response due to the interaction with the nuclear current and spin-magnetization. The latter one involves operators of the type $\vec{\sigma} \times \vec{q}$, as discussed before.

Fig. 21 shows $S_T(\omega,q)$ deduced for ^{56}Fe [60] and compared with a Fermi gas RPA plus 2p2h calculation in the local density approximation [61]. The calculation covers the nucleon-hole excitation region and shows the substantial influence of 2p2h contributions in filling the minimum around $\omega \simeq 200$ MeV. At larger energy transfers, S_T rises again towards the $\Delta(1232)$ region.

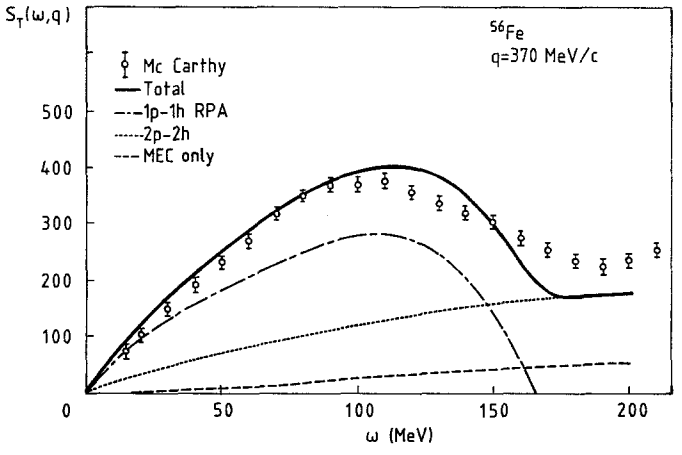

Figure 21: Transverse structure function deduced from inelastic electron scattering on ^{56}Fe [60]. The calculations [61] show the response in 1p1h RPA, 2p2h contributions, and the effect of meson exchange currents (MEC).

LECTURE 8

8. Pion-Nucleus Scattering and Related Processes

Pion-nucleus scattering (or: pion optics) divides naturally into the low energy region ($0 < T_\pi \lesssim 80$ MeV) and the $\Delta(1232)$ resonance region (80 MeV $\lesssim T_\pi \lesssim 400$ MeV), where T_π is the pion kinetic energy. The characteristic features can be illustrated already by considering the pion mean free path in nuclear matter, $\ell = (\rho\sigma)^{-1}$, where ρ is the density and σ the isospin averaged πN cross section. In the Δ resonance region, one obtains $\ell \simeq 0.5$ fm; the interaction of a pion with the nucleus is therefore surface dominated. This is to be seen in contrast with low energy scattering. There the πN interaction is weak. The mean free path is several fm, of the order of the nuclear size or larger; the π-nucleus interaction takes place all over the nuclear volume, and specific many-body corrections are important.

8.1 Low-Energy π-Nucleus Elastic Scattering

The starting point of the theory of low energy π-nucleus interactions is the optical potential, eq. (6.18). In the local density approximation, $\rho \to \rho(\vec{r})$, the first order potential becomes

$$2\omega\, U_{opt}^{(o)}(\omega,\vec{r}) = -4\pi\left[b_o(\omega)\,\rho(\vec{r}) - c_o(\omega)\,\vec{\nabla}\rho(\vec{r})\vec{\nabla}\right], \qquad (8.1)$$

where we have added an s-wave part to the leading p-wave interaction. At threshold, $b_o = 1/3(a_1 + 2a_3)$.

However, first order potentials of this type fail badly when confronted with pionic atom data and low energy cross section. Corrections of higher order in density are required. The essential ones have already been introduced: those related to pion absorption, primarily through coupling to the two-particle-two-hole continuum, and the Lorentz-Lorenz correction.

A consistent description of both pionic atom and low energy scattering can be obtained with the following potential [55,62] (for spherical N = Z nuclei):

$$U_{opt} = U^{s}_{opt} + U^{p}_{opt} , \tag{8.2}$$

where

$$2\omega\, U^{s}_{opt}(\omega,r) = -4\pi\left[b_0(\omega)\,\rho(r) + B_0(\omega)\,\rho^2(r)\right], \tag{8.3a}$$

$$2\omega\, U^{p}_{opt}(\omega,\vec{r}) = -4\pi\,\vec{\nabla}\,\frac{c(r) + C(r)}{1 + 4\pi g'\left[c(r)+C(r)\right]}\,\vec{\nabla}, \tag{8.3b}$$

where $$c(r) = c_0(\omega)\,\rho(r) \quad , \quad C(r) = C_0(\omega)\,\rho^2(r), \tag{8.3c}$$

and we have omitted for simplicity kinematic corrections of order ω/M which are non-negligible in practical calculations.

A typical calculation is presented in Fig. 22 using the parameters in table 3 [62] which also reproduce the shifts and widths of pionic atom levels. The main point to summarize the results is that many-body corrections of order ρ^2 are important. There is a strong correlation between Re C_0, which can be interpreted as the dispersive shift due to absorption effects together with binding effects, and the parameter g' representing the Lorentz-Lorenz correction. It is therefore not possible to determine either one of these parameters directly from pion elastic scattering.

The imaginary part of the optical potential at threshold and at low energy is entirely determined by pion absorption. The absorption cross section is

$$\sigma_{abs} = -\,(2\omega/q)\,\langle\phi_q|\,\mathrm{Im}\,U\,|\,\phi_q\rangle,$$

where q is the pion momentum and ϕ_q are the pion distorted waves evaluated with the full U_{opt}. Given Im B_0 and Im C_0 as in table 3, σ_{abs} comes out to be sizeable, typically more than 1/2 of the total cross sections at low energy. Both B_0 and C_0 have been evaluated in microscopic models, assuming that pion absorption takes place primarily on nucleon pairs. The calculations can then be constrained by the measurements of the $\pi d \leftrightarrow NN$ process.

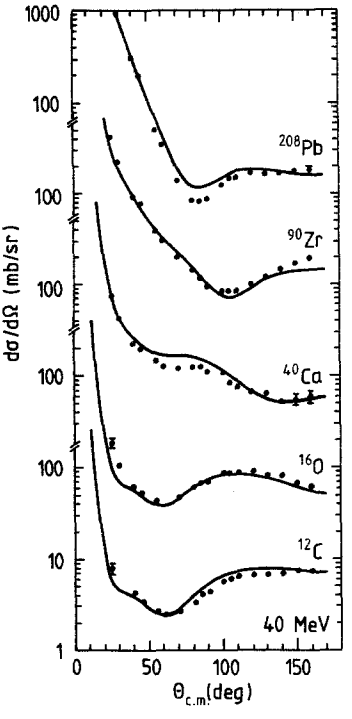

$b_o[m_\pi^{-1}]$	- 0.03	
Re $B_o[m_\pi^{-4}]$	0.0	
Im $B_o[m_\pi^{-4}]$	0.05	
$c_o[m_\pi^{-3}]$	0.23	0.23
g'	0.47	0.60
Re $C_o[m_\pi^{-6}]$	0.04	0.14
Im $C_o[m_\pi^{-6}]$	0.12	0.17

table 3: Best fit values of optical potential parameters (eq. (8.3) adjusted to pionic atom data. The two alternative sets of p-wave parameters give equivalent fits.

Figure 22: Differential cross sections for π-nucleus elastic scattering at T_π = 40 MeV. The parameters are those of table 3 and include a smooth variation from pionic atoms to 40 MeV scattering.

8.2 Scattering in the Δ-Resonance region

A characteristic feature of pion-nucleus scattering around T_π = 160 MeV is the strong diffractive structure of the differential cross section $d\sigma/d\Omega$, indicating that a large part of the scattering at resonance is simply determined by geometry. In fact, because of the Δ(1232) resonance in the elementary πN amplitude, the imaginary part of the first order (Born) scattering amplitude is very large at these energies. The scattering process is qualitatively similar to scattering from a black sphere. By analogy with optics, diffraction at the edge of the sphere of radius R leads to a characteristic pattern in $d\sigma/d\Omega$, the first minimum appearing roughly at the angle where $qR \sim \pi$.

This picture, though qualitatively correct, is too primitive however when it comes to a more quantitative discussion. The precision and abundance of data for some selected nuclei is sufficient to allow for a partial wave analysis. A prototype nucleus is ^{16}O which we shall now examine in more detail.

We denote by $F(\theta,\omega)$ the $\pi^{16}O$ scattering amplitude where ω is the pion energy in the π-nucleus c.m. system and $d\sigma/d\Omega = |F|^2$. For targets with zero spin such as ^{16}O, we have the partial wave decomposition

$$F(\theta,\omega) = \sum_{J=0}^{\infty} (2J+1)\, F_J(\omega)\, P_J(\cos\theta). \qquad (8.4)$$

that the Δ(1232), even in a nuclear environment, can be treated as quasiparticle, like the nucleon itself, specified by an effective mass and width.

The question whether such a picture works, and where are its limits, can be regarded as one of the primary motivations for investigating pion-nucleus scattering in the Δ region.

The Δ-hole model combines the basic requirement of a good first order input with a proper many-body framework for systematic improvements in the treatments of higher order corrections. The framework is that of the response function developed in Chapter 7.

The lowest order response, or optical potential, through Δ-hole intermediate states is

$$2\omega \langle \vec{q}' | U_{opt}^{(o)}(\omega) | \vec{q} \rangle = \langle \vec{q}' | H^{+}_{\pi N\Delta} G_o^{\Delta}(\omega) H_{\pi N\Delta} | \vec{q} \rangle \tag{8.7}$$

where $\vec{q}$ and $\vec{q}'$ denote in- and outgoing pion momenta, and $G_o^{\Delta}(\omega)$ is the first order Δ-hole Green's function, eq.(7.10). Iteration of G_o^{Δ} to all orders with the Δ-hole interaction $V_{\Delta h}$, i.e. the Δ-hole analogue of the spin-isospin interaction $V_{\sigma\tau}$ of eq. (6.25), gives the RPA Δ-hole Green's function G^{Δ}, which is further modified by coupling of the Δ-hole states to the two-particle-two-hole continuum etc. to account for absorptive damping. Once this is done, the pion-nucleus T-matrix is given in the form (see eq. (7.6)):

$$\begin{aligned} 2\omega \langle \vec{q}' | T(\omega) | \vec{q} \rangle &= \langle \vec{q}' | H^{+}_{\pi N\Delta} G^{\Delta}(\omega) H_{\pi N\Delta} | \vec{q} \rangle \\ &= -4\pi F(\theta,\omega). \end{aligned} \tag{8.8}$$

The full Δ-hole Green's function is a sum of terms, each characterized by a specific Δ-hole angular momentum J^{π}.

The actual calculations [5,64 - 66] all follow essentially the same basic RPA approach to the response function. They differ in the detailed treatment of Δ-hole interactions and in their (either microscopic [5,66] or phenomenological [64]) incorporation of important couplings to two-nucleon-two-hole continuum states, the ones relevant for the description of pion absorption channels.

8.4 Δ-Hole Doorway States

We proceed now to present an example of such a calculation. We point out that in the partial wave expansion of the scattering amplitude, eq. (8.4), the $J^{\pi} = 0^{+}, 2^{-}, 3^{+}, \ldots$ etc. coincides with the angular momentum and parity of the Δ-hole excitation modes. These modes are shown in Fig. 24 for $\pi^{16}O$ in terms of the partial cross sections,

$$\sigma_J(\omega) = \frac{4\pi}{q} (2J+1)\, Im\, F_J(\omega). \tag{8.9}$$

The complex F_J have been obtained for all partial waves $0 \leq J \leq 8$ in ref. [63]. Except for the $J^\pi = 0^-$ partial wave which supposedly carries a strong portion of non-resonant s-wave interactions, all partial waves with $J \leq 5$ show a resonant behaviour. However, there is a massive damping in all partial waves: the inelasticities η_J, defined by

$$\eta_J = |S_J| \qquad \text{where} \quad S_J = 1 + 2iq F_J, \tag{8.5}$$

q being the π-nucleus c.m. momentum, come down as far as $\eta_J \simeq 0.2$ for $J \leq 3$ in the kinetic energy region 100 MeV $\leq T_\pi \leq$ 180 MeV. The total cross section,

$$\sigma_{tot}(\omega) = \frac{4\pi}{q} \, Im \, F_J(\theta=0, \omega), \tag{8.6}$$

and the inelastic cross section for $\pi^{16}O$ derived from this analysis are presented in Fig. 23.

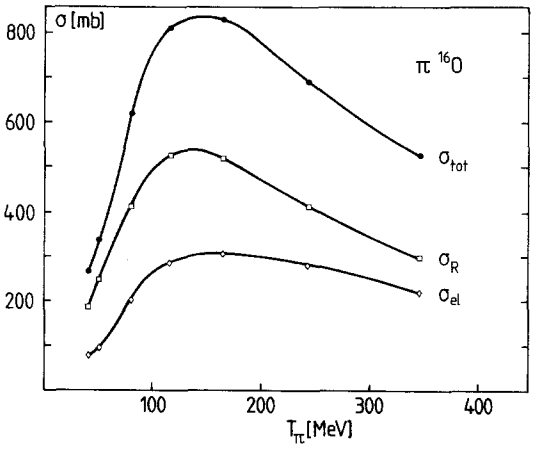

Figure 23: Total, elastic and reaction cross sections for $\pi^{16}O$ scattering (with Coulomb corrections removed) taken from the analysis of ref. [63].

About one half of the reaction cross section turns out to be related to pion absorption. The major part of the other half comes from inelastic scattering processes with knockout of one or more nucleons (such as quasifree scattering, $(\pi,\pi'N)$).

The large reactive content of the total pion-nucleus cross section is an important feature. In models where the scattering process is described by the excitation and subsequent propagation of a Δ(1232) inside the nucleus, this implies that there must be a substantial damping width experienced by the Δ(1232) in a many-body environment.

8.3 The Δ-Hole Model

The dominance of the Δ(1232) in the pion-nucleon spin-isospin-3/2 channel suggests that the basic mode of excitation at pion kinetic energies between 100 - 300 MeV is the creation of Δ-hole pairs. This is the asumption behind the Δ-hole model. It asserts

The result can be cast into a simple form by identifying each strength distribution for a given J^π with essentially one or two Δ-hole doorway states $|d_J\rangle$:

$$2\omega \langle \vec{q}' | T(\omega) | \vec{q} \rangle = \sum_{d_J} \frac{\langle \vec{q}' | H^{+}_{\pi N\Delta} | d_J \rangle \langle \tilde{d}_J | H_{\pi N\Delta} | \vec{q} \rangle}{\omega - E_J(\omega) + i\Gamma_J(\omega)/2} \,. \qquad (8.10)$$

Each Δ-hole mode of given J^π has a resonant structure, the position of the maximum moving upward with increasing J. The width of each mode is determined by several

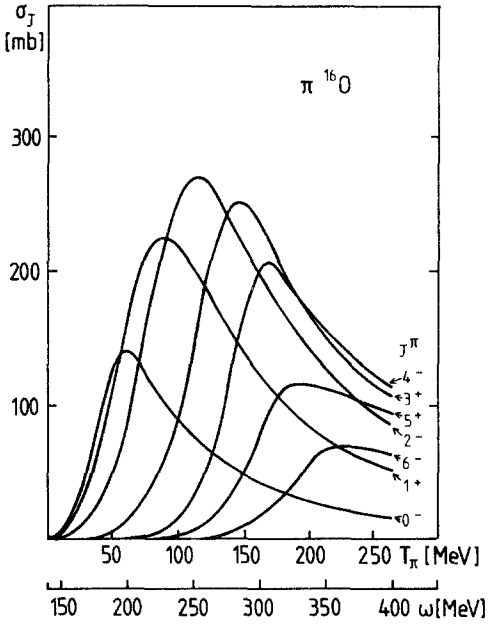

Figure 24: Distribution of Δ-hole strength as seen in pion-nucleus scattering from ^{16}O. Shown is the result of a microscopic Δ-hole calculation [5,66].

factors: (i) the $\Delta \to \pi N$ decay width, partly quenched by Pauli blocking effects, and very importantly, (ii) the absorptive channels arising from the coupling of Δ-hole to the 2N2h continuum. A special feature of the longitudinal spin-isospin response such as it is studied in pion-nucleus scattering, is the downward shift in energy of Δ-hole peaks in lower partial waves. This shift comes mainly because of the strong attraction from non-static one-pion exchange in the (direct) Δ-hole interaction, or equivalently, from the coherent multiple scattering of the pion through the nucleus. The downward shift is partly reduced by the repulsive Δ-hole interaction proportional to g'_Δ, and further influenced by dispersive shifts from absorptive channels. The latter effect is one of the reasons why it is not possible to determine g' directly from Δ-nucleus scattering. Nevertheless the Δ-hole model has been remarkably successful in its capacity to treat genuine many-body corrections to the propagation of the $\Delta(1232)$

inside a nucleus. In fact, the Δ-hole strength distributions, Fig. 24, are very close to those obtained from the partial wave analysis [63] except for the $J^\pi = 0^-$ partial wave which requires a careful treatment of s-wave πN interactions not incorporated in $H_{\pi N\Delta}$

The downward shift of Δ-hole strength in low partial waves observed in π-nucleus scattering is absent in photonuclear cross sections in the Δ-region. This is easily understood because of the dominant transverse $\gamma N\Delta$ coupling proportional to $\vec{S}^+ \times \vec{q}$ which suppresses the direct OPE Δ-hole interaction, the latter involving longitudinal operators of the type $\vec{S}^+ \cdot \vec{q}$ [67].

8.5 The Δ-Nuclear Effective Potential

One can think of all the above mentioned effects on the $\Delta(1232)$ propagation inside the nucleus as being described by a complex optical potential for the Δ. This potential will in general be non-local, because of the large distances over which the excited nuclear many-body system can propagate in space. An equivalent local potential of the form

$$V_\Delta(E,r) = W_o(E)\,\frac{\rho(r)}{\rho_o} + 2\,\vec{\ell}_\Delta \cdot \vec{s}_\Delta\; V_{LS}(r) \tag{8.11}$$

has been used successfully [64] in systematically reproducing elastic pion-nucleus data together with total absorption cross sections. (In such an approach, the Pauli blocking terms (Fock terms) are usually calculated explicitly so that their real and imaginary parts do not appear in V_Δ). The result obtained for ^{12}C and ^{16}O is

$$W_o \cong (-30 - i\,40)\ \text{MeV}, \tag{8.12}$$

almost independent on pion energy in the range T_π = 100 - 250 MeV.

Non-localities enter, at least partly, through the spin-orbit term, where $\vec{\ell}_\Delta$ and $\vec{s}_\Delta$ are the orbital angular momentum and the spin of the propagating $\Delta(1232)$. With the parametrization

$$V_{LS} = V_o^{LS}\,\mu r^2 e^{-\mu r^2} \tag{8.13}$$

and μ = 0.3 fm^{-2} the following value has been obtained for ^{16}O:

$$V_o^{LS} = (-10 - i\,4)\ \text{MeV}. \tag{8.14}$$

The size of the spin-orbit interaction for Δ's is therefore roughly comparable with that for nucleons. With inclusion of a spin-orbit term, the fit to differential cross sections improves systematically, as Fig. 25 shows. In the absence of V_{LS} the required W_o is strongly energy dependent.

The phenomenological Δ-nuclear potential is sometimes called spreading potential in order to emphasize the spreading of strength from the Δ-hole doorway states into other

inelastic channels. Its significance is that it sets the scale for the size of many-body effects related to absorption and other reactive channels. A reactive width of $\Gamma_R \sim 80$ MeV for the central partial waves ($J \leq 3$ at $T_\pi = 160$ MeV) emphasizes the importance of the partial Δ decay into channels other than $\Delta \to \pi N$ inside the nucleus. The imaginary part of W_o is actually quite well reproduced by coupling the Δ-hole states to the two-nucleon-two-hole continuum in a model constrained by the $\pi d \to pn$ absorption amplitude [5].

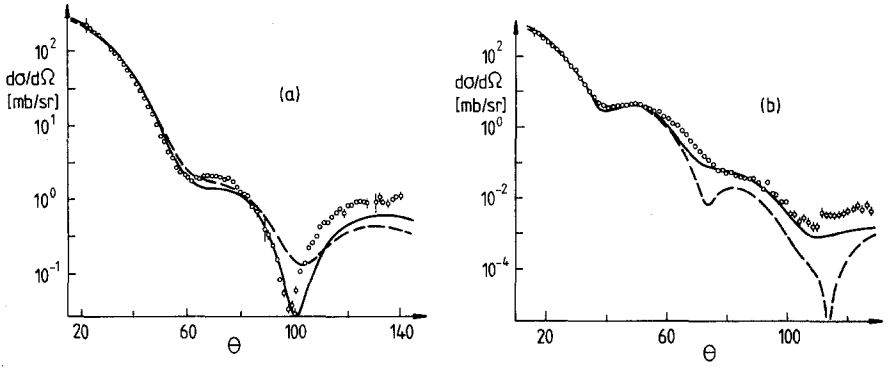

Figure 25: Δ-hole model calculation of $\pi^{16}O$ differential cross sections (Horikawa et al. [64]) showing the influence of the Δ-nucleus spin-orbit interaction (solid curve) as compared to $V_{LS} = 0$ and W_o readjusted (dashed curve). (a) $T_\pi = 114$ MeV; (b) $T_\pi = 240$ MeV.

LECTURE 9

9. Gamow-Teller and Magnetic Isovector Transitions

Substantial experimental progress has been made in the past few years, in the systematic exploration of Gamow-Teller (GT) strength by (p,n) [68] and (^{3}He, t) [69] processes, and in the investigation of magnetic transitions in a variety of nuclei using high resolution inelastic electron scattering. Both the GT strength and the magnetic transitions of low multipolarity are observed to be systematically quenched as compared to shell model expectations. Part, but not all of the quenching can be attributed to standard nuclear core polarization. The interesting question is then to what extent the unexplained parts of the quenching can be interpreted as signatures of sub-nucleonic effects, such as polarization involving virtual Δ excitations.

The (p,n) process takes advantage of the fact that at energies 100 - 200 MeV of the incoming proton, the spin-isospin dependent part of the nucleon-nucleon interaction dominates strongly over the purely isospin dependent one, thus favouring GT($\sigma\tau$) transitions over Fermi (τ) transitions. The same is true for the (^{3}He,t) reaction.

9.1 Quenching of Gamow-Teller Transitions

GT transitions are related to the nuclear axial current operator

$$\vec{A}^{\pm}(\vec{r}) = g_A \sum_{i=1}^{A} \vec{\sigma}_i \tau_i^{\pm} \delta^3(\vec{r}-\vec{r}_i). \tag{9.1}$$

The total GT strength as seen in (p,n) reactions at forward angles can be compared with the sum rule [68]

$$\frac{1}{g_A^2} \sum_n \left\{ |\langle n|\vec{A}^+(\vec{q}=0)|0\rangle|^2 - |\langle n|\vec{A}^-(\vec{q}=0)|0\rangle|^2 \right\} = 3(N-Z) \tag{9.2}$$

where the intermediate states $|n\rangle$ are purely nucleonic ones. Only $\vec{\sigma}\tau^+$ contributes to (p,n) reactions, but the τ^- part is strongly suppressed by the Pauli principle for nuclei with large neutron excess. The actual strength observed is greatly reduced as compared to eq. 9.2 . If reexpressed in terms of an effective g_A^{eff}, the ratio (g_A^{eff}/g_A) is obtained as shown in Fig. 26 [68]. The fraction of GT strength observed as compared to the sum rule is (65 ± 5)%. This includes a careful consideration of background subtractions from energies above the actual GT resonance state [71].

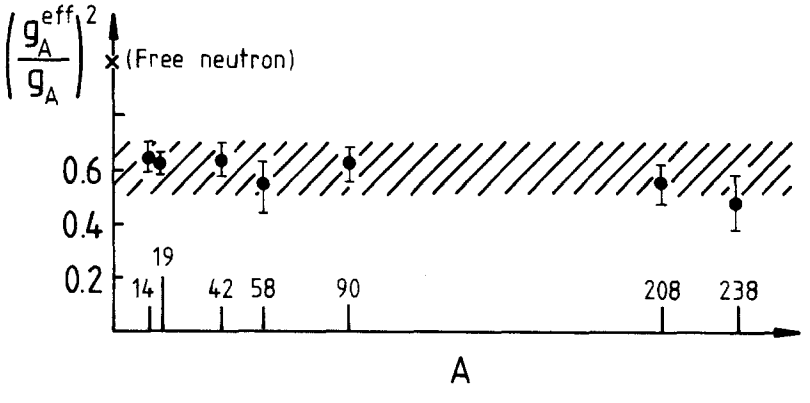

Figure 26: Fraction of Gamow-Teller sum rule strength observed in (p,n) reactions [68].

The systematics of the quenching of the axial charge g_A in nuclei for a wide range of mass numbers is a remarkable feature. We note that with $g_A = 1.26$ for a free neutron, the effective g_A in nuclei appears to be

$$g_A^{eff} = 1.02 \pm 0.03 . \tag{9.3}$$

Similar conclusions are drawn by a systematic analysis of magnetic moments and beta decays of mirror nuclei [72].

It is instructive to look back at the GT sum rule from a quark model point of view [73]. We recall that eq. (9.2) is derived for a nucleus consisting of nucleons only. The

Δ(1232) can be introduced by writing the sumrule starting at the quark level from an axial current

$$\vec{A}^{\pm} = \sum_{Q=1}^{3A} \vec{\sigma}_Q \tau_Q^{\pm} , \tag{9.3}$$

where the $\vec{\sigma}\tau^{\pm}$ now operate on the individual u and d quarks. The corresponding quark sum rule is

$$\sum_n \left\{ |\langle n| \sum_{Q=1}^{3A} \vec{\sigma}_Q \tau_Q^+ |0\rangle|^2 - |\langle n| \sum_{Q=1}^{3A} \vec{\sigma}_Q \tau_Q^- |0\rangle|^2 \right\} = 3(N-Z). \tag{9.4}$$

Note that the summation over intermediate states $|n\rangle$ necessarily involves both nucleon and Δ intermediate states, since these states just truncate all possible quark spin-isospin transitions at zero momentum transfer. If the summation over $|n\rangle$ is restricted to nucleons only, the result is (25/3)(N-Z) on the right hand side of eq. (68). By comparison with eq. (9.2), this reveals $g_A = 5/3$, the familiar constituent quark model value for g_A. We note the reduction of the quark sum rule, with Δ's included, over the nucleon sum rule (excluding Δ's) by a factor 9/25. The discussion cannot be applied to realistic situations since the model is obviously oversimplied, giving $g_A = 5/3$ instead of 1.26. Nevertheless, such considerations are useful since they illustrate the connections between nucleons and Δ's in spin-isospin excitation channels. If looked at from a quark sum rule point of view, the presence of Δ's reduces the GT sum rule, eq. (9.2), by effectively replacing g_A by $g_A^{eff} = 1$, in surprising coincidence with eq. (9.3).

9.2 Quenching of Isovector Magnetic Spin Transitions

Isovector magnetic spin transitions are related to the nuclear spin current

$$\vec{J}_M(\vec{r}) = g_M \sum_i (\vec{\sigma}_i \times \vec{\nabla}) \tau_i^3 \delta^3(\vec{r} - \vec{r}_i). \tag{9.5}$$

A similar systematics as in GT transitions is found in M1 and M2 transitions, if the observed strength is reexpressed in terms of an effective spin-g-factor, $g_M^{eff} = \gamma g_M$ in eq. (9.3) [70]. The quenching factor γ is shown in Fig. 27. This is not a model independent evaluation, since an RPA calculation has been used for reference (no sum rule of the simple type, eq. (9.2), exists for magnetic transitions).

The quenching of M1 and M2 strength by a factor $\gamma^2 \simeq 1/2$ (except for light nuclei) raises the question about common quenching mechanisms for both g_A and g_M, the corresponding operators being obtained from each other just by an isospin rotation.

Before going into a more detailed discussion of spin-isospin quenching mechanisms, it is interesting to recall the magnetic moments situation. Arima [73] has repeatedly emphasized that the systematics of renormalization effects observed in magnetic moments over a wide range of nuclei can be well accounted for by standard core polarization and tensor correlations, with only little room left for polarization effects involving the Δ(1232). In that respect, it is important to note [74 ,75] that there is a

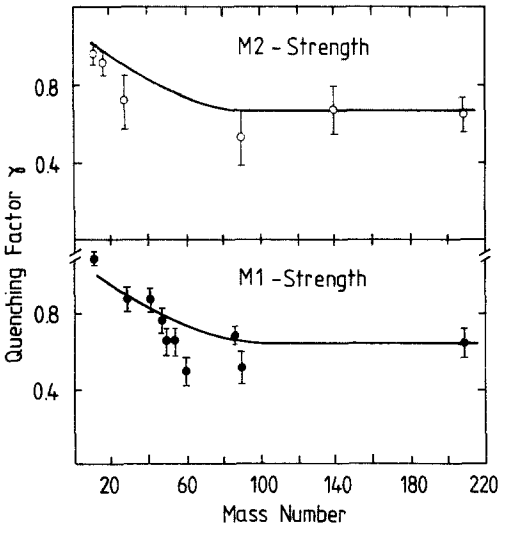

Figure 27: Quenching factor $\gamma = g_M^{eff}/g_M$ associated with the reduced M1 and M2 strength observed in (e,e') experiments (from ref. [70]).

substantial difference between magnetic moments and M1 transitions, as far as the role of the Δ(1232) is concerned. The effective magnetic dipole operator can be written as

$$\vec{\mu}_{eff} = \frac{1}{2} g_s^{eff} \vec{\sigma} + g_\ell^{eff} \vec{\ell} + \sqrt{\frac{\pi}{2}}\, g_p\, [\vec{\sigma} \times Y_2]^{[1]}, \tag{9.6}$$

where the g-factors stand for

$$g = g^{(0)} + g^{(1)} \tau_3 . \tag{9.7}$$

The contribution of eq. (9.6) to magnetic moments and reduced M1 transition matrix elements is (e.g. [75]):

$$\mu(j = \ell + 1/2) = \frac{1}{2}\left\{ g_s^{eff} + 2\ell\, g_\ell^{eff} + \frac{\ell}{2\ell+3}\, g_p \right\}, \tag{9.8a}$$

$$\mu(j = \ell - 1/2) = -\frac{1}{2}\left[\frac{2\ell-1}{2\ell+1}\right]\left\{ g_s^{eff} - 2(\ell+1)\, g_\ell^{eff} + \frac{\ell+1}{2\ell-1}\, g_p \right\}, \tag{9.8b}$$

$$\langle j' \| \vec{\mu}_{eff} \| j \rangle = (-)^{\ell + 1/2 - j'} \left[\frac{2j+1}{2(2\ell+1)}\right]^{1/2} \left(-g_s^{eff} + g_\ell^{eff} + \frac{1}{4} g_p \right). \tag{9.8c}$$

The point is that contributions from g_s and g_p appear with the same sign in diagonal matrix elements, but with opposite sign in M1 transition matrix elements. Now, Δ-hole polarization effects are shown [74,75] to contribute with opposite signs to g_s and g_p, which means that $\Delta(1232)$ effects interfere destructively in magnetic moments, whereas they add coherently in B(M1) values. Thus the place to look for possible Δ degrees of freedom is in spin transitions rather than moments.

6.3 Renormalization of Spin-Isospin Operators in Nuclei

We proceed now with a discussion of the possible sources for the quenching of spin-isospin strength in the low energy, long wavelength limit. Given a repulsive spin-isospin dependent particle-hole interaction at low momentum transfers (recall eq. (6.31)), a substantial reduction of spin-isospin strength, as compared with independent particle model exceptations, is already obtained within standard RPA with nucleons only. This is seen by recalling from eq. (7.11) that RPA introduces a "quenching factor" ε^{-1}, with

$$\varepsilon = 1 - V_{\sigma\tau} G_o^N \tag{9.9}$$

in the response function. For finite nuclei, this ε is a non-local operator [5]. Its analogue in nuclear matter, where longitudinal and transverse spin-isospin channels decouple, is a simple function of ω and q which is often referred to as the longitudinal or transverse diamesic function.

For transitions to specific final states, the screening of the perturbing operator F by the RPA polarization cloud introduces an effective operator,

$$F_{eff} = \varepsilon^{-1} F = \frac{F}{1 - V_{\sigma\tau} G_o^N} \,. \tag{9.10}$$

Since G_o^N at $\omega = 0$ goes like

$$G_o^N(\omega = o) = -2 \sum_{Nh} \frac{|Nh\rangle\langle Nh|}{\varepsilon_N - \varepsilon_h} \tag{9.11}$$

and $V_{\sigma\tau}(\omega = q = 0) = g' \vec{\sigma}_1 \cdot \vec{\sigma}_2 \, \vec{\tau}_1 \cdot \vec{\tau}_2$ with $g' > 0$, the reduction of F_{eff} with respect to F is obvious. Part of this RPA screening can simply be interpreted as an effect of ground state correlations, as shown in Fig. 28. The situation is quite different at high momentum transfers, especially in longitudinal ($\vec{\sigma} \cdot \hat{q} \, \tau^{\lambda}$ type) channels. As q increases, the attraction from the OPE part of $V_{\sigma\tau}$ sets in, and screening may be turned into antiscreening, depending on the effects of cutoffs in πNN vertex form factors.

In practical calculations, one usually truncates the particle-hole basis (the model space, or P space). Any polarization effect outside that model space (involving the residual Q space, P + Q = 1) tends to introduce additional quenching. For example, Bertsch and Hamamoto [77] find in a perturbative calculation that there is a strong mixing of the Gamow-Teller resonance with high-lying 2p2h configurations, so that a

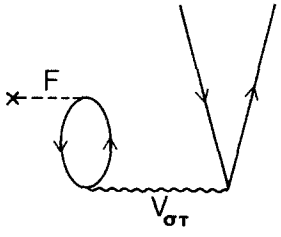

Figure 28: Quenching of spin-isospin transitions by RPA type ground state correlations. Note that by Pauli principle considerations, this affects M1 transitions but not GT transitions.

large fraction of the GT strength in ^{90}Zr is moved up to the continuum between 10 - 45 MeV, by mechanisms illustrated in Fig. 29. The tensor part of the effective interaction becomes very important in these mixings, a fact also pointed out in [73-75] tensor force effects. The Bertsch and Hamamoto result, namely that about half of the GT strength is moved to the 2p2h continuum, seems to be an overestimate, though. A careful reanalysis [76] of the GT background places upper limits ($\lesssim$ 20 %) for the strength moved into the continuum between 20 - 40 MeV.

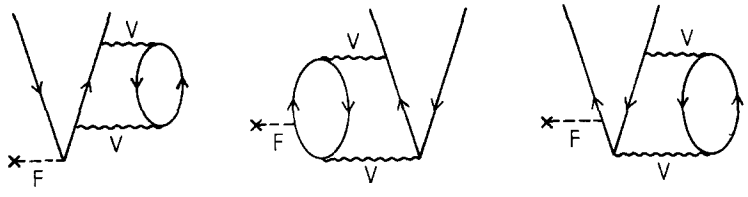

Figure 29: Three out of many diagrams involving mixings of 1p1h states with high lying 2p2h excitations.

6.4 Δ-hole induced Screening of Spin-Isospin Operators

In addition to the screening due to conventional nuclear polarization mechanisms, we expect that virtual Δ-hole excitations contribute to the quenching factor ε. We have demonstrated the existence of broad Δ-hole states at excitation energies around 300 MeV. The question is now to what extent virtual Δ-hole excitations participate in the nuclear spin-isospin response even at low energy. Suppose that all relevant conventional nucleon degrees of freedom are treated explicitly in a sufficiently large model space (P-space), such that the remaining Q-space contains all polarization effects where intrinsic $N \to \Delta$ transitions are involved. Within RPA reduced to P space, the effective spin-isospin operators incorporating Δ-hole screening effects (see Fig. 30) will now be

$$F_{eff} = \varepsilon_\Delta^{-1} F, \qquad \varepsilon_\Delta = 1 - V G_o^\Delta , \tag{9.12}$$

where V = V(Δh) is the Δ-hole interaction and G_o^Δ is the Δ-hole Green's function, eq. (7.10)

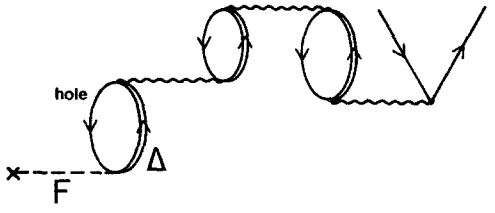

Figure 30: Screening of spin-isospin operators by virtual Δ-hole excitations within RPA.

It is instructive to discuss ε_Δ in the static long-wavelength limit for nuclear matter. The Δ-hole interaction in this limit becomes

$$V(\Delta h) = g_\Delta' \vec{S}_1 \cdot \vec{S}_2^+ \vec{T}_1 \cdot \vec{T}_2^+ , \tag{9.13}$$

where g_Δ' is the relevant Landau-Migdal parameter derived from the ΔN-interaction. The G_o^Δ at ω = 0 is proportional to $\rho/(M_\Delta - M_N)$, where ρ is the nuclear density and $M_\Delta - M_N$ is the ΔN mass difference. Carrying out spin-isospin sums, one obtains

$$\varepsilon_\Delta = 1 + g_\Delta' \lambda \frac{\rho}{\rho_o} , \tag{9.14}$$

where the density is given in units of nuclear matter density, $\rho_o = 0.17$ fm^{-3}, and the constant λ is

$$\lambda = \frac{8}{9}\left(\frac{72}{25}\right) \frac{\rho_o}{M_\Delta - M} m_\pi^{-2} . \tag{9.15}$$

The factor 72/25 is obtained if one assumes the SU(4) scaling between NN and NΔ spin-isospin transitions, in which case $\lambda \simeq 0.6$. (In the Chew-Low model, the 72/25 would be replaced by 4 and λ would be increased correspondingly.) The Δ-induced quenching factor is seen to be determined by g_Δ' in the long wavelength limit. For example, with $g_\Delta' = 0.5$ one obtains $\varepsilon_\Delta = 1.3$ at nuclear matter density, $\rho = \rho_o$. This quenching is obviously common to both GT and magnetic spin transitions. That is, the effective axial vector coupling constant and isovector spin g-factor become:

$$g_A^{eff}/g_A = g_M^{eff}/g_M = [1 + \lambda g_\Delta' \rho/\rho_o]^{-1} . \tag{9.16}$$

This Δ-hole induced screening of spin-isospin transitions has been discussed widely in the literature [78].

In finite nuclei, ε_Δ becomes a non-local operator, as discussed before, and calculations are usually performed keeping the full finite range structure of the Δ-hole interaction,

including one-pion exchange and ρ exchange. The non-local and finite range effects have two consequences, namely that the Δ-induced quenching effect depends on the nuclear mass number (quenching is less for light nuclei) and on the angular momentum J of the state considered (less quenching for large J; see ref. [5]).

The essential parameter governing the Δ-hole screening is g'_Δ. We have already mentioned that, unlike g' for nucleons, g'_Δ is subject to considerable uncertainty. In many-body schemes which start from a boson exchange model of the NN → NΔ or NΔ → NΔ interaction, exchange terms (Fig. 31b) tend to cancel direct terms (Fig. 31a) of the Δ-hole interaction [79], the cancellation being most effective in short range pieces, like exchange. The resulting g'_Δ would be small, about 0.3, hence Δ-hole quenching would not be substantial. In fact, the cancellation is complete for a zero range interaction. However, recent estimates [80] indicate that one has to carry on with the question of exchange terms along the lines of ref. [54] to include the induced interaction (Fig. 31c). In fact, diagrams (b) and (c) (taken to all orders) of Fig. 31 tend to cancel largely among themselves, leaving Fig. 31(a) as the dominant piece. In any case, this is just a limited set out of many more diagrams, and one has to raise the question how far the standard many-body framework with "elementary" nucleons and Δ exchange terms can be pushed at short distances. The Landau-Migdal framework avoids these problems by operating with the direct particle-hole interaction, Fig. 31(a) only, and assigning a phenomenological g'_Δ, including exchange, to this channel. As mentioned before, we shall strictly maintain this philosophy in the following.

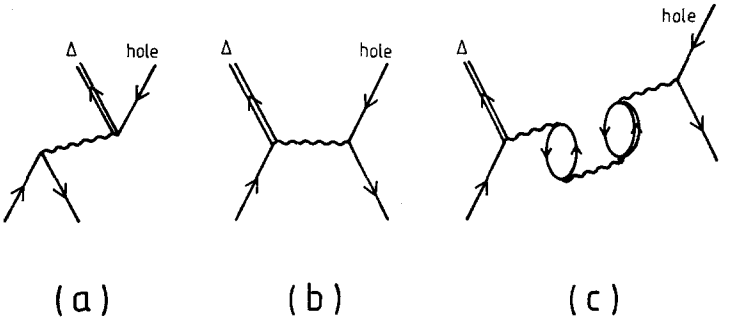

Figure 31: Direct (a) and exchange (b) pieces of the Δ-hole transition interaction. The exchange terms are screened by higher order diagrams of the type (c), the induced interaction in this channel.

LECTURE 10

9.5 A specific example: M1 Transition to the 10.2 MeV State in ^{48}Ca

This state, seen first in (e,e′) scattering [81] is by now one of the best studied examples of quenched M1 strength. According to McGrory and Wildenthal [82], this state has a relatively simple shell model structure dominated by a $f_{5/2}f_{7/2}^{-1}$ neutron-hole configuration. The wave function obtained from a full fp-shell model calculation (which defines the model space, or P space) is

$$|^{48}Ca; 1^+\rangle = 0.89\,|\nu f_{5/2} f_{7/2}^{-1}; 1^+\rangle + 0.11\,|\nu f_{7/2} f_{5/2}^{-1}; 1^+\rangle\,, \qquad (9.17)$$

plus additional small admixtures of more complicated configurations. The dominant neutron-hole component makes this a favourable case for studying renormalization effects of the spin g factor. A pure $f_{7/2} \to f_{5/2}$ single particle transition using the unrenormalized value for g_s gives $B(M1)\uparrow = 12\,\mu_N^2$, whereas the experimental value is $(3.9 \pm 0.3)\mu_N^2$ [81]. Using the wave function, eq. (9.17), the $B(M1)\uparrow$ comes down to $7.3\mu_N^2$. A major fraction of this quenching comes from 2p-2h ground state correlations of the type shown in Fig. 28. Such 2p-2h correlations are also incorporated in standard RPA calculations (Suzuki, Krewald and Speth, 1981), where $B(M1)\uparrow = 8\mu_N^2$ is found. The additional quenching of about $1\mu_N^2$ is due to more complicated many-particle-many-hole effects not present in RPA.

The effect of pionic exchange currents is small, but acts to increase the effective g_s by $\lesssim 10$ % (Kohno and Sprung [78]). This discussion indicates that subtle cancellations are involved (Towner and Khanna [74]). It shows also, however, that it is difficult to obtain a B(M1) much less than $7\text{-}8\mu_N^2$ from ground state correlations and mesonic exchange currents. Another factor 1.5 - 2 reduction is still required.

Now, if g'_Δ is sufficiently large, Δ-hole screening is a candidate for supplying a good fraction of the remaining quenching. This is shown in Fig. 32 (Härting et al. [78]; see also ref. [83]), where the Δ-hole screening (on top of the McGrory-Wildenthal pf-shell model space) has been calculated with a Δ-hole force consisting of π and ρ exchange plus a Landau-Migdal zero range interaction proportional to g'_Δ, the parameter which has been varied. The full non-local structure of the diamesic function ε_Δ as well as the proper angular momentum projection is kept in this calculation. The Chew-Low ratio $f_\Delta/f = 2$ has been used here. (For comparison with calculations using the constituent quark model value $f_\Delta/f = \sqrt{72/25}$, multiply g'_Δ in Fig. 14 by a factor 1.4). Note that for finite nuclei such as ^{48}Ca, there is a mixing of transverse and longitudinal parts of the Δ-hole interaction even though the probing M1 field is purely transverse. As a consequence the attraction from OPE reduces somewhat the quenching from g'_Δ alone, an effect observable in the limit $g'_\Delta = 0$.

Next, we wish to consider the M1 form factor of the same 10.2 MeV state in ^{48}Ca, which has been measured by Steffen et al. [84]. We do this in several steps, starting from

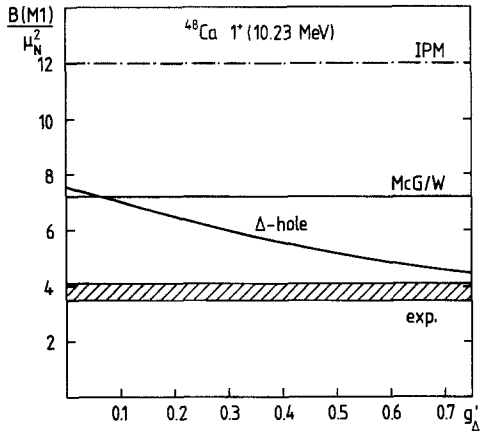

Figure 32: B(M1)↑ value for ^{48}Ca(1^+). IPM: result for pure $(f_{5/2}\, f_{7/2}^{-1})$ neutron-hole configuration. McG/W: result of full fp-shell model calculation (McGrory and Wildenthal, [82]). Δ-hole: result including Δ-hole screening in addition to McG/W as a function of the Δ-hole Landau-Migdal parameter g'_Δ.

the McGrory-Wildenthal wave function, eq. (9.17), and introducing Δ-hole screening as in Fig. **30.** The calculation here is comparable to the large space RPA calculation of Suzuki et al. [78]). They use a similar Δ-hole interaction, but with inclusion of exchange terms for π and ρ exchange, which is equivalent to choosing a much reduced g'_Δ (in the Landau Fermi Liquid picture). However, they also observe that they have to add in by hand a $\delta g'_\Delta > 0$ in order to fit the energy of the 1^+ state. This $\delta g'_\Delta$ compensates for the reduction of g'_Δ obtained by explicit calculation of exchange terms. In our calculation, exchange terms are systematically omitted, for reasons given earlier.

The full fp-shell model space has the advantage that it includes many-particle-many-hole configurations not present in RPA. But it omits nucleon core polarization effects outside that model space. We have included such effects at least partly by incorporating all RPA type nucleon-hole polarization diagrams outside P-space to all orders. The different steps of the calculation are shown in Fig. **33a**. Note that the quenching effect due to Δ-hole and nucleon-hole polarization is q-dependent, reflecting the q-dependence of the Δ-hole interaction from π and ρ exchange.

Meson exchange current effects increase the M1 form factor up to the first maximum by about 10 %. Consequently, for $g'_\Delta = 0.6$, there is still room for an additional renormalization of the isovector spin-g factor by about 10 %. Fig. **33b** shows the result [85] when all effects are included, together with a $g_s^{eff} = 0.9\, g_s$. This latter factor may represent, for example, second order core polarization processes of the type, Fig. **29**, not included within RPA.

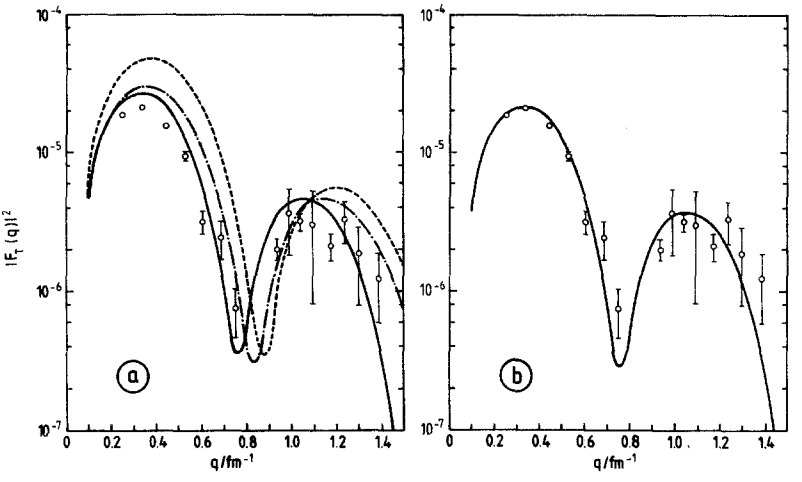

Figure 33: DWBA-calculations of the transverse form factor for ^{48}Ca(e,e') (1^+; 10.2 MeV). (a) Dashed curve: McGrory-Wildenthal fp-shell model result; dash-dotted curve: effect of Δ-hole screening, with $g'_\Delta = 0.6$; solid curve: additional effect of RPA-type nucleon-hole polarization outside the fp-shell; (b) curve obtained from solid curve of (a) by adding meson exchange currents and using $g_s^{eff} = 0.9\ g_s$ (from ref. [85]; exp. data: ref. [84]).

In summary, the above example gives indications for Δ(1232) induced quenching, but has also evinced the difficulties in discriminating such effects against "standard" nuclear properties, such as ground state correlations and core polarization. A Δ-hole induced reduction of the isovector g_s and g_A by 30 - 35 % can be obtained for values $g'_\Delta = 0.5 - 0.6$ of the Δ-hole Landau-Migdal parameter. We note that while this Δ-hole quenching is common to both GT and M1 transitions, ground state correlations act differently in both cases, namely, they are reduced for GT transitions in neutron rich nuclei. Meson exchange currents contribute relatively little to the renormalization of g_s (an increase by less than 10 % for the ^{48}Ca example). The situation here is different from that in very light nuclei, where pion exchange dominate and Δ(1232) effects are relatively small (see Chapter 4).

10. Hyperons in Nuclei

10.1 Strangeness Exchange Reactions

We have discussed mechanisms to create a Δ(1232) in a nucleus by pion-induced processes The main motivation for doing so was to study interactions of the Δ with surrounding nucleons. In a similar way, kaon beams have been used to implant Λ and Σ hyperons in nuclei in order to investigate their interactions with a nuclear environment.

The Λ and Σ have strangeness S = - 1. They are produced in the following strangeness exchange reactions on nucleons:

$$K^- + N \rightarrow \Lambda + \pi, \tag{10.1}$$

$$K^- + N \rightarrow \Sigma + \pi. \tag{10.2}$$

The (K^-,π^-) reaction on nuclei has been used extensively to form Λ and Σ hypernuclei [87 - 89].

Consider first the Λ production process, eq. (10.1). A particularly interesting feature of the kinematics is that for a K^- momentum of 500 MeV/c, the recoiling Λ is produced with zero momentum (recoilless production, see table 4), if the pion is detected under forward angles. This has important consequences for Λ hypernucleus produced under these

K^- momentum [MeV/c]	0	100	300	500	700	900
Λ momentum [MeV/c]	250	190	70	0	40	80

table 4: Recoil momentum in $K^-n \rightarrow \pi^-\Lambda$ with pions detected at angle 0^o.

kinematical conditions. It means that the neutron in a given shell model orbit will be replaced preferentially by a Λ carrying the same orbital quantum numbers.

10.2 Spectroscopy of Λ-Hypernuclei

We consider here the Λ-hypernuclear excitation spectra in $^{12}_{\Lambda}C$ and $^{16}_{\Lambda}O$ obtained with the (K^-,π^-) reaction and shown in Fig. 34. The spectra are plotted as a function of the mass difference $M_{HY} - M_A$ of the hypernucleus and the target nucleus. Also plotted is the binding energy B_Λ, and the Λ-nuetron mass difference is indicated for orientation.

The interesting point to note is first that the spectrum looks very much like one which would follow from a simple shell model picture: the neutron is removed from the p-shell of carbon and oxigen and replaced by a Λ which occupies any one of the p- or s-shell orbits available to it in an assumed Λ-nucleus average potential. Now, in ^{12}C, only the $p_{3/2}$ neutron shell is occupied, whereas in ^{16}O, a neutron in either $p_{3/2}$ or $p_{1/2}$ orbit can be replaced by a Λ. A comparison of $^{16}_{\Lambda}O$ and $^{12}_{\Lambda}C$ as in Fig. 34 therefore permits to extract not only the depth of the average Λ-nucleus potential, but also the strength of the Λ-nucleus spin-orbit interaction. A detailed phenomenological analysis [90] yields the following results: if the Λ-nucleus single particle potential is written as

$$V_\Lambda(r) = W_o \frac{\rho(r)}{\rho_o} + V_o^{LS} \frac{d}{dr}\left(\frac{\rho(r)}{\rho_o}\right) \frac{\vec{\ell}\cdot\vec{\sigma}}{r}, \tag{10.3}$$

then

$$W_o = (-32 \pm 2)\ MeV, \tag{10.4}$$

$$V_o^{LS} = (4 \pm 2)\ MeV\,fm^2. \tag{10.5}$$

Thus the central potential depth for a Λ is about half as deep as that of a nucleon, while the Λ spin-orbit coupling is only about 1/4 or less compared to the spin-orbit force of nucleons in nuclei.

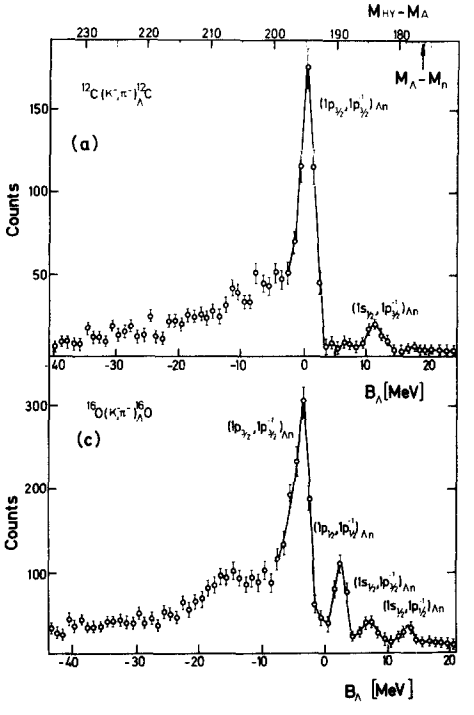

Figure 34: Spectra obtained from the (K^-,π^-) reaction [88] on ^{12}C and ^{16}O at a kaon momentum of 715 MeV.

10.3 The Hyperon-Nucleon Spin-Orbit Interaction

The size of the spin-orbit force is evidently an interesting piece of information, since it reflects properties of the hyperon-nucleon effective interaction at relatively short distances. Several attempts have been made to relate the results, eqs. (10.4-5), to properties of the underlying two-body interaction.

One such approach starts from a relativistic boson exchange model and relates the central potential depth to the spin-orbit force in a Dirac-Hartree-Fock calculation [91,92]. With constraints set by the potential well depth and spin-orbit splitting in nuclei, and with SU(3) applied to hyperon-nucleon interactions, one finds values of W_o and V_o^{LS} in good agreement with the empirical values.

The smallness of the ΛN spin-orbit force comes as a natural result also in simple quark rearrangement plus gluon exchange models [93]. The Λ is a combination of u, d and s quark in such a way that (ud) couple to a spin and isospin singlet. Therefore the spin-orbit interaction due to exchange of u or d quarks vanishes for the diagonal $\Lambda N \to \Lambda N$ interaction where no s quark is exchanged. The contribution from $\Lambda N \to N\Lambda$

exchange processes is small.

However, the same naive quark model predicts a value 4/3 for ratio of ΣN to NN spin-orbit forces in nuclei [93]. In contrast, boson exchange models generally suggest a small Σ-nucleus spin-orbit coupling [94,95]. Experimental data [89] on Σ-hypernuclei can be interpreted assuming an average Σ-nucleus potential depth of about - 30 MeV. Unfortunately, the data seem so far not to be sufficiently accurate to deduce an unambgibuous Σ-nucleus spin-orbit potential; nevertheless there are claims [96] in favour of an interpretation with a large V_{LS} for Σ's.

Whether this apparent discrepancy between meson exchange and simple quark models leads us to the limits of the boson exchange phenomenology is a question of vital importance In any case, one would wish that Σ-hypernuclear data become available in the future at a level of accuracy such that this problem can be sorted out.

REFERENCES

[1] Proc. 8th Int. Conf. on High Energy Physics and Nuclear Structure, Vancouver 1979, Nucl. Phys. A 335 (1980)
[2] Proc. 9th Int. Conf. on High Energy Physics and Nuclear Structure, Versailles 1981, Nucl. Phys. A 372 (1982)
[3] Mesons in Nuclei, Vol. I-III, M. Rho and D.H. Wilkinson, eds., North-Holland Publ. Co. (1979)
[4] A.W. Thomas and R.H. Landau, Phys. Reports 68 (1980)121
[5] E. Oset, H. Toki and W. Weise, Phys. Reports 83 (1982) 281
[6] F. Lenz and E. Moniz, Adv. in Nucl. Phys. 13 (1983)
[7] M. Lacombe et al., Phys. Rev. C 23 (1981) 2405; R. Vinh Mau, in: Mesons in Nuclei, Vol. I, M. Rho and D. Wilkinson, eds., North-Holland, Amsterdam (1979)
[8] A.D. Jackson, D.O. Riska and B.J. Verwest, Nucl. Phys. A 249 (1975) 397; G.E. Brown and A.D. Jackson, The Nucleon-Nucleon Interaction, North-Holland, Amsterdam (1976)
[9] K. Holinde, Phys. Reports 68 (1981) 121; R. Machleidt, in: Quarks, Mesons and Isobars in Nuclei, R. Gurardiola and A. Polls, eds., World Scientific, Singapore (1983)
[10] K. Erkelenz, Phys. Rep. 13 (1974) 191
[11] M.M. Nagels, T.A. Rijken and J.J. de Swart, in: Few Body Systems and Nuclear Forces, Vol. I (1978), Lecture Notes in Physics, Springer (1978)
[12] W. Grein and P. Kroll, Nucl. Phys. A 338 (1980) 332
[13] A. Chodos, R.L. Jaffe, C.B. Thorn and V. Weisskopf, Phys. Rev. D 9 (1974) 3471; A. Chodos, R.L. Jaffe, K. Johnson and C.B. Thorn, Phys. Rev. D 10 (1974) 2599;
[14] A. Chodos and C.B. Thorn, Phys. Rev. D 12 (1975) 2733
[15] G.E. Brown and M. Rho, Phys. Lett. 82 B (1979) 177; G.E. Brown, M. Rho and V. Vento, Phys. Lett. 84 B (1979) 383; V. Vento et al., Nucl. Phys. A 345 (1980) 413
[16] G.A. Miller, A.W. Thomas and S. Théberge, Phys. Lett. 91 B (1980) 192; Phys. Rev. D 22 (1980) 2823; A.W. Thomas, Adv. in Nucl. Phys. 13 (1983) 1
[17] W. Weise, in: Quarks, Mesons and Isobars in Nuclei, R. Guardiola and A. Polls, eds. World Scientific (1983), p. 146
[18] R. Tegen, R. Brockmann and W. Weise, Z. Physik A 307 (1982) 339; R. Tegen, M. Schedl and W. Weise, Phys. Lett. 125 B (1983) 9
[19] T.D. Lee, Particle Physics and Introduction to Field Theory, Harwood Publ., London (1981) R. Friedberg and T.D. Lee, Phys. Rev. D 18 (1978) 2623
[20] R. Goldflam and L. Wilets, Phys. Rev. C 25 (1982) 1951
[21] M. Brack, Phys. Rev. D 27 (1983) 1950
[22] Y. Nambu and G. Jona-Lasinio, Phys. Rev. 122 (1961) 345, 124 (1961) 246
[23] R. Brockmann, W. Weise and E. Werner, Phys. Lett. 122 B (1983) 201; V. Bernard, R. Brockmann, M. Schaden, W. Weise and E. Werner, Nucl. Phys. A 412 (1984) 349
[24] S.J. Brodsky and G.P. Lepage, Phys. Scripta, 23 (1981) 945; S.J. Brodsky, in: Quarks and Nuclear Forces, Springer Tracts in Mod. Phys. 100 (1982) 81
[25] P.A.M. Guichon, G.A. Miller and A.W. Thomas, Phys. Lett. 124 B (1983) 109
[26] R. Tegen and W. Weise, Z. Physik A 314 (1983) 357
[27] E. Oset, R. Tegen and W. Weise, Univ. Regensburg preprint TPR-84-1 (1984)
[28] T.E.O. Ericson and M. Rosa-Clot, Nucl. Phys. A 405 (1983) 497
[29] J. de Kam, Z. Physik A 310 (1983) 113; M. Schedl, private communication
[30] G.E. Brown and W. Weise, Phys. Reports 22 (1975) 279
[31] M. Chemtob and M. Rho, Nucl. Phys. A 163 (1971) 1
[32] D.O. Riska, in: Mesons in Nuclei, Vol. II, M. Rho and D. Wilkinson, eds., North-Holland (1979)
[33] H. Miyazawa, Progr. Theor. Phys. 6 (1951) 801; J.I. Fujita and M. Ichimura, in: Mesons in Nuclei, M. Rho and D. Wilkinson, eds., North-Holland (1979), p. 625; T. Yamazaki, ibido, p. 651
[34] J.A. Lock and L.L. Foldy, Ann. of Phys. 93 (1973) 276
[35] M. Bernheim et al., Phys. Rev. Lett. 46 (1981) 402

[36] J. Hockert, D.O. Riska, M. Gari and G. Hoffmann, Nucl. Phys. A 217 (1973) 14
[37] H. Arenhövel, Nucl. Phys. A 374 (1982) 521 c
[38] R.A. Brandenburg et al., Phys. Rev. Lett. 32 (1974) 325
[39] J.M. Cavedon et al., contribution 9th Int. Conf. High Energy Physics and Nuclear Structure, Versailles (1981)
[40] E. Hadjimichael, R. Bornais and B. Goulard, Phys. Rev. Lett. 48 (1982) 583
[41] G. Höhler, Landolt-Börnstein, Numerical Data ..., Vol. I/9b2, p. 279, Springer (1983)
[42] M. Ericson, Ann. of Phys. 63 (1971) 562; T.E.O. Ericson, in: Proc. Conf. on Common Problems in Low- and Medium-Energy Physics, B. Goulard and F.C. Khanna, eds., Plenum (1979)
[43] A.L. Fetter and J.D. Walecka, Quantum Theory of Many-Particle Systems, McGraw-Hill (1971)
[44] N.C. Mukhopadhyay, H. Toki and W. Weise, Phys. Lett. 84 B (1979) 35
[45] A.B. Migdal, Rev. Mod. Phys. 50 (1978) 107
[46] G.E. Brown and W. Weise, Phys. Reports 27 (1976)1
[47] W. Dickhoff, H. Müther and A. Faessler, Phys. Rev. Lett. 49 (1982) 1902
[48] M. Anastasio and G.E. Brown, Nucl. Phys. A 285 (1977) 516
[49] W. Weise, Nucl. Phys. A 278 (1977) 4021
[50] A.B. Migdal, Theory of Finite Fermi Systems, Interscience (1967)
[51] J. Speth, E. Werner and W. Wild, Phys. Reports 33 (1977) 127
[52] J. Speth, V. Klemt, J. Wambach and G.E. Brown, Nucl. Phys. 343 (1980) 382; P. Ring and J. Speth, Nucl. Phys. A 235 (1974) 315
[53] S.O. Bäckman, A.D. Jackson and O. Sjöberg, Nucl. Phys. A 321 (1979) 10
[54] W.H. Dickhoff et al., Nucl. Phys. A 369 (1981) 445; Phys. Rev. C 23 (1981) 1154
[55] M. Ericson and T.E.O. Ericson, Ann. of Phys. 36 (1966) 383
[56] S. Borshay, G.E. Brown and M. Rho, Phys. Rev. Lett. 32 (1974) 787
[57] W. Weise, Phys. Lett. 117 B (1982) 150
[58] A. Arima, T. Cheon, K. Shimizu, H. Hyuga and T. Suzuki, Phys. Lett. 122 B (1983)126
[59] A. Arima and H. Hyuga, in: Mesons in Nuclei, Vol. II, M. Rho and D. Wilkinson, eds., North Holland (1979)
[60] J.S. McCarthy, Nucl. Phys. A 335 (1980) 27c
[61] W. Alberico, M. Ericson and A. Molinari, Nucl. Phys. A 386 (1982) 412, and CERN preprint
[62] K. Stricker, J. Carr and H. McManus, Phys. Rev. C 22 (1980) 2043
[63] S. Ciulli, H. Pilkuhn and H.G. Schlaile, Z. Phys. A 302 (1981) 45
[64] M. Hirata, F. Lenz and K. Yazaki, Ann. of Phys. 109 (1977) 16; M. Hirata, J. Koch, F. Lenz and E.J. Moniz, Ann. of Phys. 120 (1979) 205; Y. Horika, M. Thies and F. Lenz, Nucl. Phys. A 345 (1980) 386 F. Lenz, M. Thies and Y. Horikawa, Ann. of Phys. 140 (1982) 266
[65] K. Klingenbeck, M. Dillig and M.G. Huber, Phys. Rev. Lett. 41 (1978) 387; Phys. Rev. C 22 (1980) 681
[66] W. Weise, Nucl. Phys. A 278 (1977) 402 E. Oset and W. Weise, Phys. Lett. 77 B (1978) 159; Nucl. Phys. A 319 (1979) 477; A 358 (1981) 163c;
[67] W. Weise, Nucl. Phys. A 358 (1981) 163c; J.H. Koch, NIKHEF preprint (1983)
[68] C. Gaarde et al., Nucl. Phys. A 369 (1981) 258; C.D. Goodman, Nucl. Phys. A 374 (1982) 241c
[69] C. Ellegard et al., Phys. Rev. Lett. 50 (1983) 1745
[70] A. Richter, Nucl. Phys. A 374 (1982) 177c
[71] F. Osterfeld, Phys. Rev. C 26 (1982) 762
[72] B. Buck and S.M. Perez, Phys. Rev. Lett. 50 (1983) 1975
[73] J. Delorme, M. Ericson and P. Guichon, Phys. Lett. 115 B (1982) 86
[74] A. Arima and H. Hyuga, in: Mesons in Nuclei, Vol. II, M. Rho and D.H. Wilkinson, eds., North-Holland (1979)
[75] I.S. Towner and F.C. Khanna, Nucl. Phys. A 399 (1983) 334
[76] R.D. Lawson, Phys. Lett. 125 B (1983) 255
[77] J. Rapaport, Proc. IUCF Workshop on "Interactions between Medium Energy Nucleons in Nuclei", preprint, Ohio University (1982)
[78] G.F. Bertsch and I. Hamamoto, Phys. Rev. C 26 (1982) 1323

[79] M. Ericson, A. Figureau and C. Thévenet, Phys. Lett 45 B (1973) 19;
R. Rho, Nucl. Phys. A 231 (1974) 493;
K. Ohta and M. Wakamatsu, Nucl. Phys. A 234 (1974) 445;
I.S. Towner and F.C. Khanna, Phys. Rev. Lett. 42 (1979) 51;
E. Oset and M. Rho, Phys. Rev. Lett. 42 (1979) 47;
H. Toki and W. Weise, Phys. Lett. 97 B (1980) 12;
W. Knüpfer, M. Dillig and A. Richter, Phys. Lett. 95 B (1980) 349;
G.E. Brown and M. Rho, Nucl. Phys. A 372 (1981) 397;
A. Bohr and B. Mottelson, Phys. Lett. 100 B (1981) 10;
A. Härting, W. Weise, H. Toki and A. Richter, Phys. Lett. 104 B (1981) 261;
T. Suzuki, S. Krewald and J. Speth, Phys. Lett. 107 B (1981) 9;
M. Kohno and D. Sprung, Phys. Rev. C 25 (1982) 297;
R.D. Lawson, Phys. Lett. 125 B (1983) 255
[80] A. Arima, T. Cheon, K. Shimizu, H. Hyuga and T. Suzuki,
Phys. Lett. 122 B (1983) 126
[81] G.E. Brown, K. Nakayama and J. Speth, private communication and preprint
[82] W. Steffen, R. Benz, H. Gräf, A. Richter, E. Spamer, O. Titze and W. Knüpfer,
Phys. Lett. 95 B (1980) 23
[83] J.B. McGrory and B.H. Wildenthal, Phys. Lett. 103 B (1981) 173
[84] W. Weise, Nucl. Phys. A 396 (1983) 373c
[85] W. Steffen, H. Gräf, A. Richter, A. Härting, W. Weise, U. Deutschmann, G. Lahm
and R. Neuhausen, Nucl. Phys. A 404 (1983) 413
[86] A. Härting, M. Kohno and W. Weise, Nucl. Phys. A (1984), in print
[87] B. Povh, Ann. Rev. Nucl. Sci 28 (1978) 1
[88] W. Brückner et al., Phys. Lett. 79 B (1978) 157
[89] R. Bertini et al., Phys. Lett. 90 B (1980) 375
[90] A. Bouyssy, Nucl. Phys. A 290 (1977) 324; Phys. Lett. 91 B (1980) 15
[91] R. Brockmann, Phys. Rev. C 18 (1978) 1510;
R. Brockmann and W. Weise, Phys. Rev. C (1977)
[92] R. Brockmann and W. Weise, Phys. Lett. 69 B (1977) 167;
Nucl. Phys. A 355 (1981) 365
[93] H.J. Pirner, Phys. Lett. 85 B (1979) 190
[94] R. Brockmann, Phys. Lett. 104 B (1981) 256
[95] C.B. Dover and A. Gal, BNL preprint (1982)
[96] B. Povh, Progr. in Part. and Nucl. Phys. 8 (1982) 325